AD-A166 803   ELECTROSTATIC HAZARDS OF URETHANE PACKED FUEL TANKS(U)   1/1
AIR FORCE WRIGHT AERONAUTICAL LABS WRIGHT-PATTERSON AFB
OH   T C HILLMAN ET AL. MAR 86 AFWAL-TR-82-2022
UNCLASSIFIED   F/G 13/12   NL

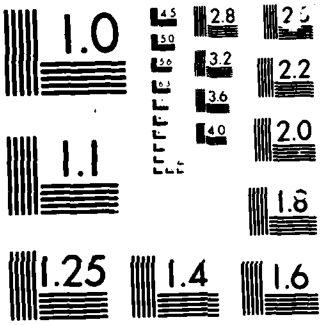

MICROCOPY CHART

2

AFWAL-TR-82-2022

ELECTROSTATIC HAZARDS OF URETHANE PACKED FUEL TANKS

Thomas C. Hillman
Jon R. Manheim
George A. Spencer

Fire Protection Branch
Fuels and Lubrication Division

March 1986

Final Report for Period March 1977 - April 1978.

Approved for Public Release; Distribution Unlimited

AERO PROPULSION LABORATORY
AIR FORCE WRIGHT AERONAUTICAL LABORATORIES
AIR FORCE SYSTEMS COMMAND
WRIGHT-PATTERSON AIR FORCE BASE, OHIO 45433-6563

NOTICE

This report has been reviewed by the Office of Public Affiars (ASD/PA) and is releasable to the National Technical Information Service (NTIS). At NTIS, it will be available to the general public, including foreign nations.

This technical report has been reviewed and is approved for publication.

ROBERT G. CLODFELTER, Chief
Fire Protection Branch
Fuels and Lubrication Division
Aero Propulsion Laboratory

FOR THE COMMANDER

Robert D. Sherrill

ROBERT D. SHERRILL, Chief
Fuels and Lubrication Division
Aero Propulsion Laboratory

UNCLASSIFIED

SECURITY CLASSIFICATION OF THIS PAGE *(When Data Entered)*

REPORT DOCUMENTATION PAGE	READ INSTRUCTIONS BEFORE COMPLETING FORM
1. REPORT NUMBER AFWAL-TR-82-2022	2. GOVT ACCESSION NO. AD-A166 803 3. RECIPIENT'S CATALOG NUMBER
4. TITLE *(and Subtitle)* ELECTROSTATIC HAZARDS OF URETHANE PACKED FUEL TANKS	5. TYPE OF REPORT & PERIOD COVERED Final Report for Period March 1977 - April 1978
	6. PERFORMING ORG. REPORT NUMBER
7. AUTHOR(s) Thomas C. Hillman* Jon R. Manheim George A. Spencer*	8. CONTRACT OR GRANT NUMBER(s)
9. PERFORMING ORGANIZATION NAME AND ADDRESS Aero Propulsion Laboratory (AFWAL/POSH) Air Force Wright Aeronautical Laboratories Wright-Patterson AFB OH 45433-6563	10. PROGRAM ELEMENT, PROJECT, TASK AREA & WORK UNIT NUMBERS Program Element 62203F Project 3048 Work Unit No. Task 304807 30480787
11. CONTROLLING OFFICE NAME AND ADDRESS Aero Propulsion Laboratory (AFWAL/POSH) Air Force Wright Aeronautical Laboratories Wright-Patterson AFB OH 45433-6563	12. REPORT DATE March 1986
	13. NUMBER OF PAGES 95
14. MONITORING AGENCY NAME & ADDRESS *(if different from Controlling Office)*	15. SECURITY CLASS. *(of this report)* Unclassified
	15a. DECLASSIFICATION DOWNGRADING SCHEDULE

16. DISTRIBUTION STATEMENT *(of this Report)*

Approved for public release; distribution unlimited.

17. DISTRIBUTION STATEMENT *(of the abstract entered in Block 20, if different from Report)*

18 SUPPLEMENTARY NOTES

*ASD/ENFEF
Wright-Patterson AFB OH 45433

19. KEY WORDS *(Continue on reverse side if necessary and identify by block number)*

Charge Density
Charge Generation
Charge Relaxation
Charging Tendency
Conductivity Additive
Electrostatic Discharge
Field Strength
Polyurethane Foam
Static Electricity

20 ABSTRACT *(Continue on reverse side if necessary and identify by block number)*

An experimental investigation has been carried out to determine the primary factors that have contributed to recent aircraft electrostatically induced ground refueling fire incidents. It was found that the explosion suppression open pore polyurethane fuel tank foams along with the charging characteristics of the JP-4 fuel resulted in charge accumulation and electrostatic spark discharging. The polyurethane foams accumulated charge due to their highly resistive nature (blue, 10^{15} ohm-cm; red, 10^{14} ohm-cm; yellow, 10^{14} ohm-cm;

DD FORM 1473 1 JAN 73 EDITION OF 1 NOV 65 IS OBSOLETE

UNCLASSIFIED

SECURITY CLASSIFICATION OF THIS PAGE *(When Data Entered)*

20. Abstract (cont)

and orange, 10^{13} ohm-cm). The fuel flow rate and velocity entering the tank and impinging on the open pore polyurethane foam directly affected the magnitude of the charge separation which was occurring. The number of refuelings that had taken place also was a critical factor due to its effect on charge accumulation/discharge frequency levels. The last major variable intestigated was pro-static (Gulf-178) and conductivity improving (Shell ASA-3) fuel additives. The Gulf-178 additive dramatically increased the levels of charge separation and accumulation taking place along with a reversal in the polarity of charge. The Shell ASA-3 fuel additive eliminated the aircraft ground refueling electrostatic discharge hazard by decreasing the level of charge accumulation.

FOREWORD

This effort was sponsored by the Aero Propulsion Laboratory, Air Force Wright Aeronautical laboratories and the Aeronautical Systems Division at Wright-Patterson Air Force Base under Project 3048, "Fuels, Lubrication, and Fire Protection," Task 304807, "Aerospace Vehicle Fire Protection." Mr J. R. Manheim of the Air Force Wright Aeronautical Laboratories, and Mr T. C. Hillman and Lt G. A. Spencer of the Aeronautical Systems Division were the engineers responsible for this in-house work. The report covers research accomplished from March 1977 through April 1978.

The authors wish to acknowledge the contributions of Mr M. A. Arstingstall and Mr D. J. Foster for their support in fabricating and operating the test rig. Finally, we would like to express our appreciation to Miss A. K. Eldridge for her assistance in preparing the report.

TABLE OF CONTENTS

LIST OF ILLUSTRATIONS

LIST OF ILLUSTRATIONS (Concluded)

LIST OF TABLES

SECTION I

INTRODUCTION

Reticulated polyurethane explosion suppression foams have been used in United States Air Force fuel tanks since the late 1960's. These foams protect fuel tanks from combustion overpressures by serving as a heat sink to reduce combustion flame temperatures and by quenching flames to limit the amount of fuel vapors from burning. Although these reticulated materials provide low weight, full time fuel tank protection, they can also generate hazardous levels of electrostatic charge. Due to the electrically nonconducting nature of the foams, charge accumulation levels high enough to produce spark discharges have resulted. During the period from December 1974 to November 1977, the Air Force experienced eight fuel tank fires caused by electrostatic spark discharges igniting the fuel-air mixture in the fuel tank ullage (Appendix E). Although the foams in many of these cases were the cause of the fires, the foams prevented any structural damage within the fuel tank. Nevertheless, due to the serious nature of this problem and lack of pertinent electrostatic test data, the Air Force initiated a number of contractual programs and a joint Air Force Wright Aeronautical Laboratories/Aeronautical Systems Division (AFWAL/ASD) in-house program to resolve the aircraft ground refueling hazard.

The objective of the joint in-house program was to study the effects certain fuel system variables had on the electrostatic hazard during ground refueling operations. The following variables were evaluated in this program:

1. Polyurethane reticulated explosion suppression foams
2. Fuel flow rate and velocity
3. Fuel pro-static additive
4. Fuel conductivity improvement additive

By studying these electrostatic variables, it was believed that the elimination of hazardous ground refueling operations could be obtained by the addition or elimination of certain fuel additives and/or by redesigning internal fuel tank configurations to reduce the electrostatic discharge problem.

SECTION II

TEST FACILITY DESCRIPTION

The electrostatic tests were conducted in Rm 101, I-Bay, Bldg 71B, Wright-Patterson AFB OH 45433-6563. The area is designed for hazardous tests and can withstand a 3.4 KPa (0.5 psig) overpressure. The test facility is equipped with a 9070 Kg (10 ton) cardox system, a ventilation system, a closed circuit surveillance television, vapor detectors, a water spray system, and a fuel/water moat area.

The test tank used in this program is illustrated in Figure 1. The tank has inside dimensions of 43 cm x 89 cm x 137 cm (17" x 35" x 54") and a volume capacity of 526 liters (139 gallons). The material used to construct the test tank was 304 stainless steel. The test tank was constructed to withstand an overpressure of 276 KPa (40 psi) with a safety factor of two. Seven 10-cm (4-inch), 150-pound ASA flanges are attached to the test tank with three flanges located on the top, three on the bottom, and one on the right side. Six of these flanges had Teflon^R covers permitting instrumentation and equipment to be isolated from the test tank. The right side of the tank had a plexiglas^R flange as the cover. This plexiglas^R flange made it possible to observe the entire inlet nozzle and the foam voided area where fuel impingement occurred. The left side of the test tank had a plexiglas^R window with dimensions 5 cm x 58 cm x 102 cm (2" x 23" x 40") and was used to observe the fuel height in the tank. The test tank was isolated from ground by eight 5-cm x 10 cm diameter (2" x 4" diameter) Teflon^R cylindrical blocks. The tank could be evacuated and dry nitrogen or air added to it.

The materials tested in this program included the reticulated polyester and the polyether urethane foams (Reference 1). These reticulated foams will subsequently be referred to as blue for the polyethers, and red, yellow, or orange for the polyester foams. The polyether foam is manufactured as a light blue fine pore, 10 pores per centimeter (PPcm; 25 PPI), and a dark blue coarse pore, 6 PPcm (15 PPI). The coarse pore dark blue foam was not tested in this program. The polyester foams consisting of red (10 PPcm; 25 PPI), yellow (6 PPcm; 15 PPI), and orange (4 PPcm, 10 PPI) were tested on a limited basis. Pertinent properties of the reticulated foams are given in Table 1 and Appendix A. The foam configuration and dimensions used in this program are illustrated in Figure 2. As can be seen from Figure 2, in the

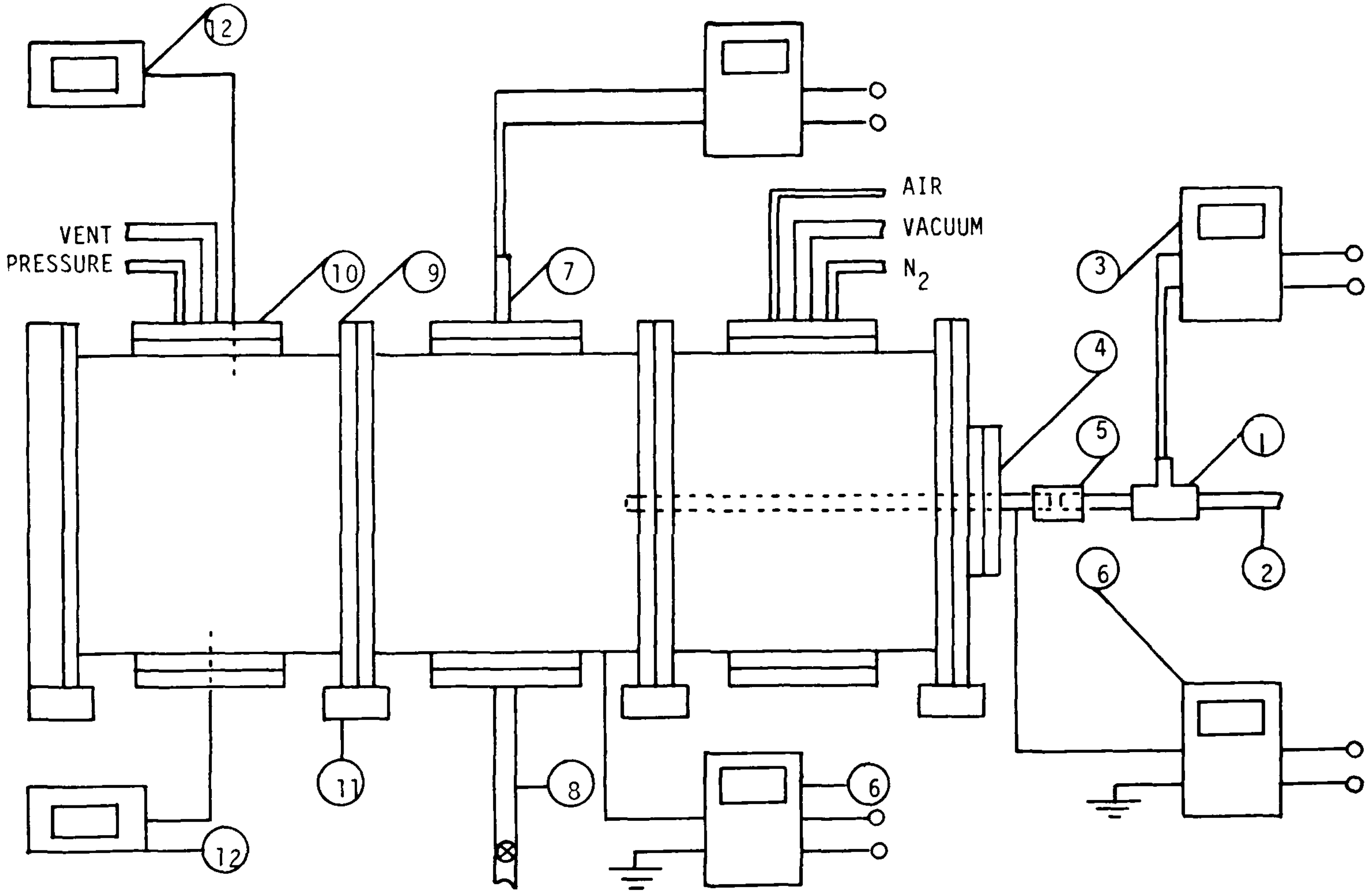

1. Turbine Flowmeter
2. Inlet Nozzle
3. Frequency Converter
4. Plexiglas® Flange
5. Teflon® Fitting
6. Electrometer
7. Field Strength Probe
8. Drain Line
9. Pressure Chamber
10. Teflon® Flange
11. Teflon® Blocks
12. Thermocouple Indicator

Figure 1. Fuel Tank Test Apparatus

TABLE 1

PHYSICAL PROPERTIES AND CHARACTERISTICS OF POLYURETHANE FOAMS (REFERENCE 1)

Property	Requirement				
	Type I	Type II	Type III	Type IV	Type V
Color	Orange	Yellow	Red	Dk. Blue	Lt. Blue
Avg. Density -g/lit (lbs/ft^3)	29.6 (1.85)	21.3 (1.33)	21.3 (1.33)	21.3 (1.33)	21.3 (1.33)
Nominal Porosity-PPCm (PPI)	4 (10)	6 (15)	10 (25)	6 (15)	10 (25)
Avg. Air Pressure Drop-NM of water (Inches of Water)	6.045 (0.238)	4.699 (0.185)	7.366 (0.290)	4.699 (0.185)	7.366 (0.290)
Fuel Displacement (Vol. %)	3.0(Max)	2.5(Max)	2.5(Max)	2.5(Max)	2.5(Max)
Fluid Retention (Vol. %)	2.5(Max)	2.5(Max)	4.5(Max)	2.5(Max)	4.5(Max)
Avg. Vol. Increase After JP-4 Fuel Age (Vol. %)	5	5	5	12	12
Extractable Materials (Wt. %)	3.0(Max)	3.0(Max)	3.0(Max)	3.0(Max)	3.0(Max)
Tensile Strength-KPa [psi]	103(Min) [15(Min)]	103(Min) [15(Min)]	103(min) [15(Min)]	69(Min) [10(Min)]	103(Min) [15(Min)]
Ultimate Elongation (%)	220(Min)	220(Min)	220(Min)	100(Min)	100(Min)
Tear Resistance-N/m [lbs/inch]	876(Min) [5(Min)]	876(Min) [5(Min)]	876(Min) [5(Min)]	525(Min) [3(Min)]	525(Min) [3(Min)]
Constant Deflection Compression Set (%)	30(Max)	35(Max)	35(Max)	30(Max)	30(Max)

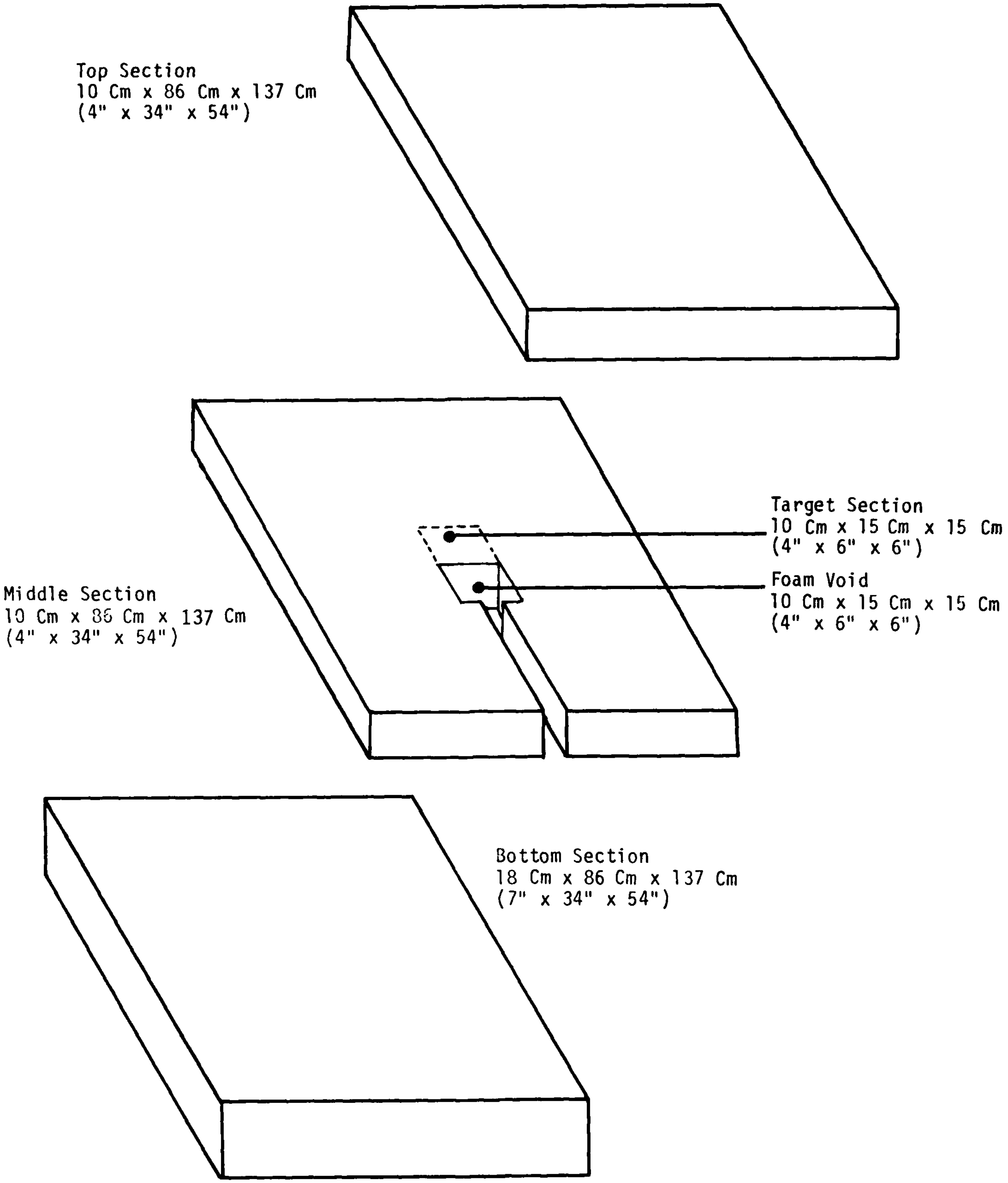

Figure 2. Fuel Tank Urethane Foam Configuration

center of the middle section was a 10 cm x 15 cm x 15 cm foam void area and a 10 cm x 15 cm x 15 cm target foam. For tests requiring new foams, only the target foam section was replaced with new foam while the top, middle, and bottom sections remained unchanged. This procedure provided a reduction in "turn-around" time and foam material consumption. This procedure was also used for tests conducted with polyester urethane foams (red and orange); however, because of the significant differences in resistivity values among red, orange, and blue foams, data obtained from these tests may not represent the case where fuel tanks are completely packed with red and orange foams. These tests were conducted to determine qualitative charge separation differences between polyester and polyether foams when fuel impinged upon them and were not intended to be comprehensive.

Two inlet nozzles were constructed of 304 stainless steel 1.9 cm (0.75") tubing with an inside diameter of 1.7 cm (0.667"). Attached to the end of one inlet nozzle was a 0.95 cm (0.375") orifice. The second inlet nozzle did not have an orifice attached to the end of it. The inlet nozzles extended 48 cm (19") into the right side of the test tank and were 23 cm (9") from the bottom of the test tank. The target foams were located approximately 13 cm (5") in front of the inlet nozzles, thus permitting JP-4 to impinge directly onto the target foam during testing.

The instrumentation used for this in-house study is illustrated in Figure 1. Their outputs were recorded with a Honeywell oscillograph. A Monroe field strength meter was used for monitoring the level of charge accumulation resulting from the filling of the test tank with JP-4 fuel. The field strength probe was centrally located on the top of the test tank. This measurement probe was isolated from the test tank by a Teflon^R fitting. Test tank field strength calibration tests were conducted to determine the effects that foam charging and field strength meter probe location would have on the measured value. This included investigating the effects of target foam location to determine where the maximum charge accumulation levels reside with reference to the centrally mounted field strength probe. The result dictated the target foam design illustrated in Figure 2. It was also found (using an uniform charge distribution source) that erroneous field strength measurements would result if the probe was not mounted flush with the test tank's ceiling. Therefore, the field strength probe mounting procedure was critical to prevent the probe from disturbing the electric field generated within the test tank (Reference 2).

In Figure 1 the inlet nozzle is shown isolated from the test tank by a plexiglas^R window and from the fuel transfer system by a Teflon^R fitting. The test tank was also isolated from the fuel transfer system, other test equipment, and earth ground by Teflon^R flanges and blocks. The isolated inlet nozzle and test tank made it possible to detect discharges occurring in the test tank and to measure any charge relaxation/generation with 602 Keithley electrometers. During certain tests the 602 Keithley electrometer, attached to the inlet nozzle, was replaced with a Tektronix oscilloscope which had storage capability. The oscilloscope was used to measure the amount of charge transferred to the inlet nozzle during a spark discharge.

The temperature of the test fuel was controlled by a self-contained mobile fuel conditioning unit. The fuel conditioner had two 380 liter (100 gallon) insulated tanks and was capable of controlling the fuel temperature from -29 to 38°C (-20 to 100°F). Based on aircraft electrostatic incidents and the flammability characteristics of JP-4 fuel, tests were conducted in the -1 to 4.5°C (30 to 40°F) temperature range.

The test tank ullage and fuel temperatures were measured with copper-constantan (TYPE T) thermocouples. During test the flow rate of the fuel was measured with a turbine flowmeter. The fuel was pumped from the fuel conditioner to the test tank by a positive displacement Moyno rotary screw pump. The pump had a maximum flow capability of 7 m^3/hr (30 GPM) with a discharge pressure of 650 KPa (80 psig). Once the fuel passed through the pump, it entered a charge relaxation chamber (i.e., straight pipe with corona discharge probes immersed in the fuel to bleed off the charge) and then an A.O. Smith charge density meter. The charge density meter measured the amount of charge per unit volume of fluid. During testing the charge density of the fuel was purposely kept low by reducing the number of expansions, contractions, and bends in the piping system, and also by not utilizing any types of charging media such as fuel filters. The charge density of the fuel remained in the range of ± 1 microcoulomb per cubic meter ($\mu C/m^3$) during testing. By ensuring that only minimal charge separation was occurring in the piping system, the charge separation which did take place could be attributed to the fuel impinging upon the foam.

The electrical conductivity of the test fuel was measured in accordance with ASTM-D-3114 and the fuel charge generating tendency was measured in accordance with the procedures developed by Exxon Research and Engineering. The descriptions and procedures for the charge tendency testing are contained in Appendix B and Reference 3.

SECTION III

RESULTS AND DISCUSSION

Before presenting the results of testing, a discussion is needed concerning the measurement techniques used in this program. The primary evaluation criteria used were the presence and number of spark discharges which occurred during a test, or the maximum field strength measured during a test, or both. During a typical test, the field strength measuring probe, which was located at the top of the test tank, measured the electrical field created by both positive charges (residing on the foam) and negative charges (residing on/in the fuel). When the field strength meter indicated a positive polarity reading, this probe primarily saw the charge on the foam. When the reading was negative, the probe was seeing the negatively charged fuel. As a test progressed, the electrical field measured at the top of the tank would initially increase to read a positive maximum and then change polarity to read a negative maximum (since the fuel level was closer to the measurement probe). The positive maximum was always greater in magnitude than the negative maximum reading. Thus, the maximum field strength data reported in Appendix C is the positive field strength readings recorded during testing. (This discussion is not applicable to the Gulf-178 additive tests [Tests 103-140] which had a negative field strength recording for the entire test.) A representation of the field strength for a typical test is shown in Figure 3.

As can be seen from the figure, a spike in the field strength measurement was observed at the beginning of each test. Although it occurred in almost every test, the source of the spike was never identified. Its magnitude was typically greater than that of the maximum positive field strength reading. However, since the nature and source of this spike could not be quantified, it was not used in this analysis.

Based on the field strength calibration tests, the area in front of the inlet nozzle is the area where the greatest charge separation and accumulation occurred. When a fueling test would begin, the field strength meter would primarily see some fraction of the residual charge on the foam in this area. As the test continued, the field strength at the top of the test tank increased in magnitude due to charge migration (from the area when the charge resides on the foam toward the field strength probe) and increasing charge density at the impingement area from

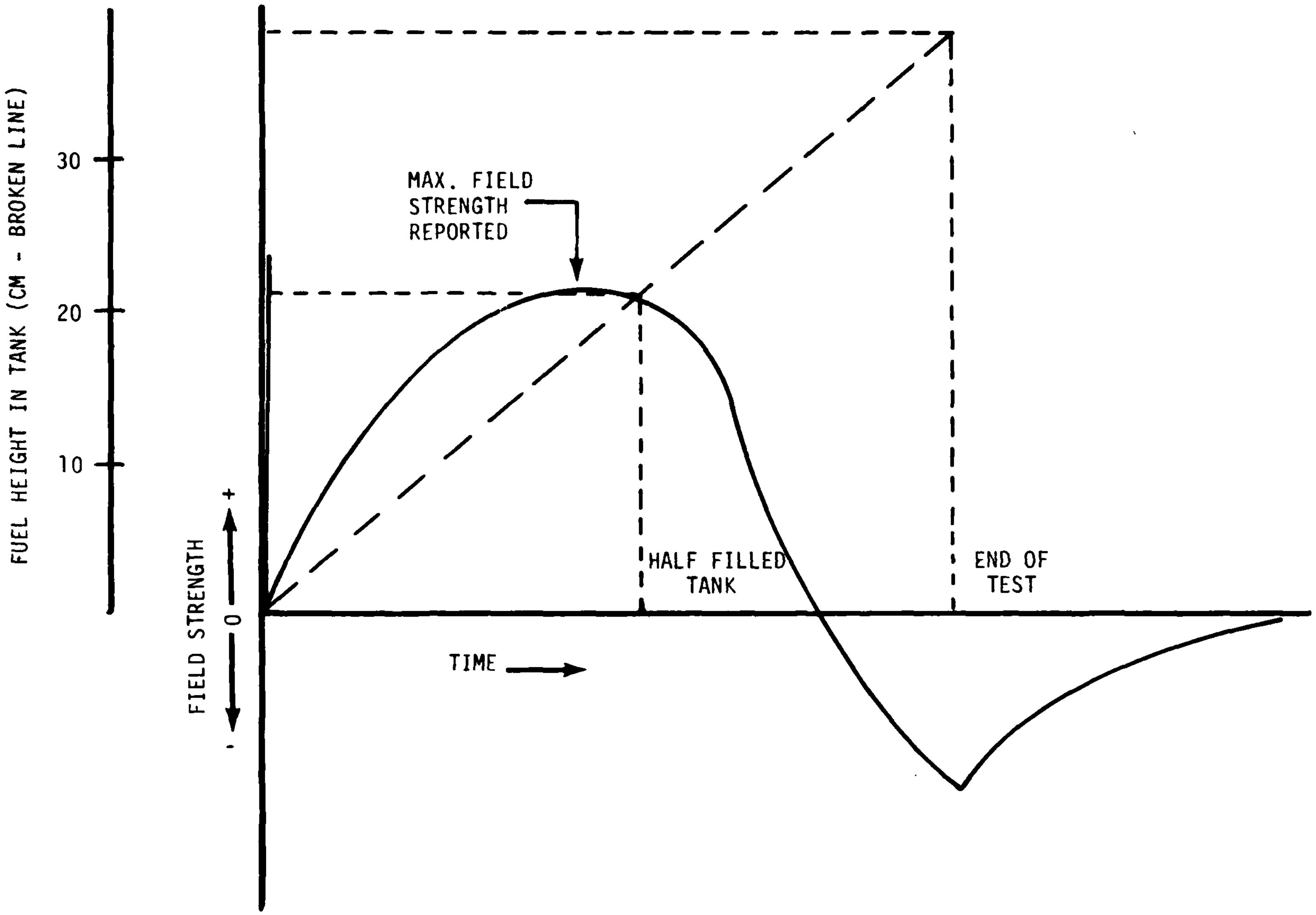

Figure 3. Illustration of Field Strength During Typical Test

additional charge separation. When the oppositely charged fuel reached and covered the pocket of charge on the foam, the field which the field strength meter saw changed. As the fuel level approached the top of the test tank, the field strength reading approached a negative polarity maximum. Some possible reasons why the magnitude of the negative reading was less than the positive reading include greater recombination of charges between the fuel and foam and greater charge relaxation of the fuel through the test tank's electrometer to ground (note, the fuel is approximately one order of magnitude less resistive than the blue foam).

The occurrence of a spark discharge is dependant upon discharge gap distance, electrode geometry (i.e., the geometry of the object which holds the charge and the geometry of the object which the charge is transferred to), electrode material composition, permittivity of the environment, as well as, localized field strength (Reference 10). It was found that after changing the target foam sections, a large amount of data scatter occurred. At times discharges were frequent, and other times there were no discharge activities under the same test configuration. This can be attributed to changing the spark breakdown gap distance each time the target foam is replaced. One would expect that if spark discharges were not occurring, higher charge accumulation levels (field strengths) would result when the same test configuration was tested (i.e., when one test had discharges and another did not). This was difficult to verify, though, due to the number of changing variables. However, it was observed that for a given test, when discharge activity was present, the field strength measurement would reach some constant value and cease to increase. Apparently, the spark discharges hindered the measured field strength from increasing in magnitude above this value. The field strength reading at which this occurred varied from test to test. Therefore, if discharge activity was occurring, one could not use the field strength measurement alone to quantify a hazard. The presence and number of discharges had to be addressed also, to determine if the discharge activity was affecting the measured field strength. Note that the field strength value measured at the top of the test tank is highly dependant upon system geometry and distance of the residual charge to the field strength measuring head, and that these measurements should not be construed as the field strengths required for charged polyurethane foam to break down air. Based on these findings, it becomes apparent that the presence and number of discharges and field strength measurements are not necessarily the best criteria for quantifying an electrostatic hazard when explosion suppression foams are being studied. However, due to the lack of any better techniques, these were the ones used.

Not only did the field strength measurement change polarity when the fuel level was in the same plane as the inlet nozzle and the target foam section (approximately 21 cm from the bottom of the test tank), any subsequent discharge activity which may have been occurring also ceased. As the fuel level covered the target foam area, several events were thought to happen: (1) the charge generation rate changed due to changing flow patterns; (2) the field strength measured at the top of the tank began seeing the negatively charged fuel over the positively charged foam; and (3) discharges occurring around the inlet nozzle ceased due to changing permittivities, greater charge recombination between the fuel and foam, and greater charge relaxation of the foam through the less resistive fuel.

While performing baseline testing, an interesting observation was made. The streaming current from the inlet nozzle was equal (within the errors of measurement) and opposite in polarity to the test tank's relaxation current. This indicated that the charge created by fuel flowing through the inlet nozzle relaxed to ground through the test tank as quickly as it was generated. However, this does not account for the charge separation taking place at the fuel-foam impingement point. This additional generation should be accounted for in the test tank's relaxation current measurement; however, it was not. When a refueling simulation was performed without polyurethane foam in the test tank and with a similar fuel (i.e., from the same fuel batch) as that used during the foam evaluation testing, the same trends in streaming and relaxation currents were noted (same magnitude as that measured with foam and still equal and opposite). This observation again leads to the conclusion that only the charge created by the inlet nozzle relaxes through the test tank to ground, and negligible amount of charge generated by the fuel-foam impingement relaxes. Recombination could account for this, but there is measurable (and substantial) charge accumulation on the foam. Thus, there should be additional charge relaxation. This phenomenon has not been explained as of yet. Furthermore, it makes it extremely difficult to use the streaming or relaxation currents to assess any electrostatic hazard.

The small-scale electrostatic test results are discussed in the appendices, while the large-scale test results will be discussed in this section in the following order (see Appendix C for test data):

1. Baseline JP-4 Fuel Tests (Tests 1 through 87)
2. Shell ASA-3 Conductivity Additive Testing (Tests 88 through 102)
3. Gulf-178 Pro-Static Additive Testing (Tests 103 through 129)
4. Shell ASA-3 and Gulf-178 Additive Testing (Tests 130-140)

1. BASELINE JP-4 FUEL TESTS

The objective of the baseline fuel tests was to study the effects of fuel flow rate/velocity and foam impingement on the electrostatic discharge phenomena.

a. Conductivity/Charge Tendency Fuel Properties

The JP-4 fuel used throughout the program met military specification MIL-T-5624K with the exception of additive anti-icing, corrosion inhibitor, etc.) and thermal stability (coker tube color equals three whereas MIL-T-5624K specifies a coker tube color of less than three) requirements. The required military additives were deliberately excluded from the fuel to ensure that a specialized case due to certain types of additives was not obtained (i.e., only the electrostatic properties associated with a neat JP-4 were to be assessed). The thermal stability requirement for the fuel concerns the residue deposited when the fuel's temperature and pressure are increased.

Throughout this report, the term "used fuel" will be mentioned. This term refers to the number of times the fuel was pumped into the test tank containing the polyurethane foam and will be referred to as fuel number. Properties of the "unused" JP-4 fuel batch (fuel number 1) used in the program are given in Table 2.

There has been some indication (Reference 4) that a fuel with low electrical conductivity and a high charge generating tendency (based on Exxon Mini-Static Charge Generating Tendency Test, Appendix B) would increase the likelihood of spark discharging during refueling operations. The charge generating Tendency apparatus,

TABLE 2

CHARACTERISTICS OF JP-4 TURBINE FUEL

COMPOSITION

ASTM METHOD						
D974	Acidity, Total (mg KOH/g)			.	0	0
D1319	Aromatics (Vol. %)		8	.	3	
D1319	Olefins (Vol. %)		1	.	0	
D1219	Sulfur, Mercaptan (Wt. %)			.	0	0
	Sulfur, Total (Wt. %)			.	0	4

VOLATILITY

D86	Distillation Initial BP(°C)				5	7
	10% Rec (°C)				8	8
	20% Rec (°C)			1	0	2
	50% Rec (°C)			1	4	0
	90% Rec (°C)			2	0	2
	Final BP (°C)			2	3	0
	Residue (%)		1	.	0	
	Loss (%)		1	.	0	
	Recovery at 204°C (%)	9	1	.	0	
D287	Gravity, API (16°C)	5	5	.	7	
D323	Reid Vapor Pressure (KPa @37.8°C)	1	7	.	9	

COMBUSTION

D1405	Aniline - Gravity Prod. 58°C	7	5	7	5	
D1322	Smoke Point	2	8	.	0	
D1655	Smoke-Volatility Index	6	6	.	2	

CONTAMINANTS

D381	Existent Gum (mg/100ml)		2	.	8	
D2276	Particulates (mg/liter)		0	.	1	
D1094	Water Reaction Vol. Chg. (ml)	0	0	.	0	
D1094	Water Reaction Ratings		1		1	
D2550	WSIM	9	4			

OTHER TESTS

D2386	Freezing Point (°C)		B	-	5	8
D130	Copper Strip (2 hr. at 100°C)	1	A			
D1660	Coker ΔP (mm Hg)		0	.	0	
D1660	Coker Tube Color	#	3			
	Anti-Icing (Vol. %)			.	0	3
D2276	Filtration Time @23°C	7 Min.				
D3114	Conductivity (pS/m)		7	.	8	3

however, incorporates a "Type 10" Facet filter paper for its charge separation medium; whereas, during an Air Force aircraft refueling operation, the largest proportion of charge separation takes place where the fuel strikes the reticulated polyurethane foams (i.e., the foam is the charge separation medium). It was believed that the amount of charge separation which occurred from a fuel was not only a function of the fuel but also the charging medium involved (Reference 5). Therefore, charging characteristics of a fuel could not be characterized using the Exxon Mini-Static Test (MST) when polyurethane foams were being studied. This could not be verified, though. Figures 4 and 5 illustrate that as the charging tendency of the fuel increased (as determined by the Exxon MST), the maximum field strength measurements and discharge activities measured during large scale fuel flow simulations tests remained somewhat constant. However, Figures 6 and 7 indicate otherwise. Figure 6 illustrates that the field strength measurement during large scale refueling simulations remained independent of MST charging tendency; however, Figure 7 indicates that the discharge activity did indeed significantly increase. These two sets of figures completely contradict each other. Kirklin (Reference 6) and Leonard and Affens (Reference 7) concluded that charge generation of fuel is dependent upon the charge separation media (foam vs. Type 10 paper), and that no correlation existed between the charging properties of the foam and filter paper. However, a correlation could not be established or disproved during these refueling simulations using the number of discharges which occurred during a test and the maximum field strength measurements as criteria for indicating a fuel's charging property in conjunction with foam.

Figures 8 and 9 illustrate the effects of used fuel on the conductivity and charge generating tendency (TYPE 10 Facet filter paper). Table 3 provides the test numbers and data to illustrate this result. As can be seen in Figure 8, the conductivity of the fuel varies from 2.9 to 8.8 picosiemens per meter (pS/m) and appears to vary in an irregular manner with repeated use of the JP-4 fuel batch. Though temperature did vary from 11 to 20°C (52 to 68°F) during the measurement of the fuel conductivity, the increase in temperature did not appear to produce the irregular pattern as can be seen from Table 3. It has not been determined whether this phenomena is due to the sampling and measuring techniques (Reference 8) or due to actual fuel flow/foam testing. Others (Reference 9) have also observed fuel conductivity changes and have attributed these changes to the absorption of impurities by the fluid during repeated blue foam impingement testing.

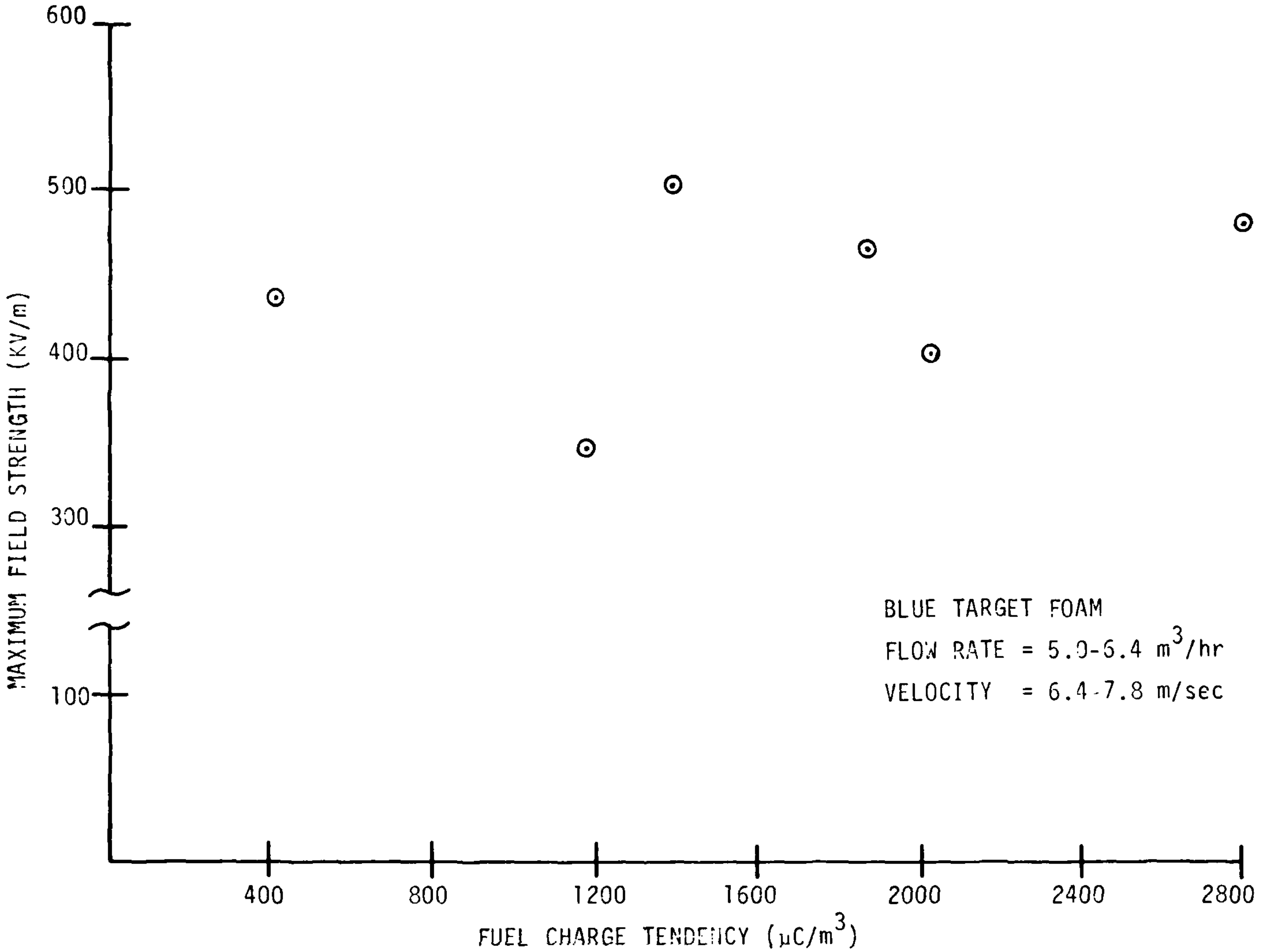

Figure 4. Maximum Field Strength Using 1.7 Cm Inlet vs. Charging Tendency of JP-4 Fuel

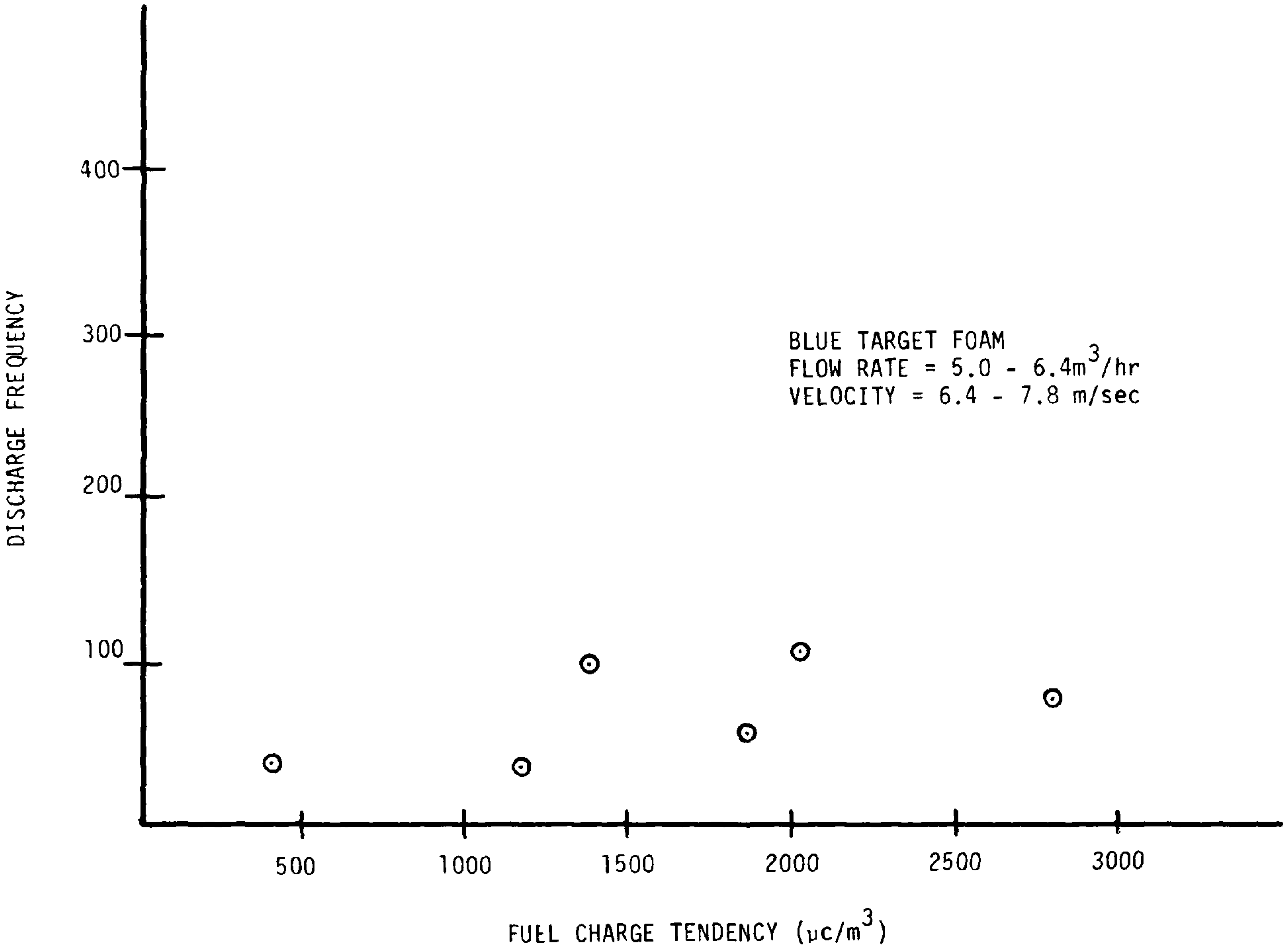

Figure 5. Discharge Activity Using 1.7 Cm Inlet vs. Charging Tendency of JP-4 Fuel

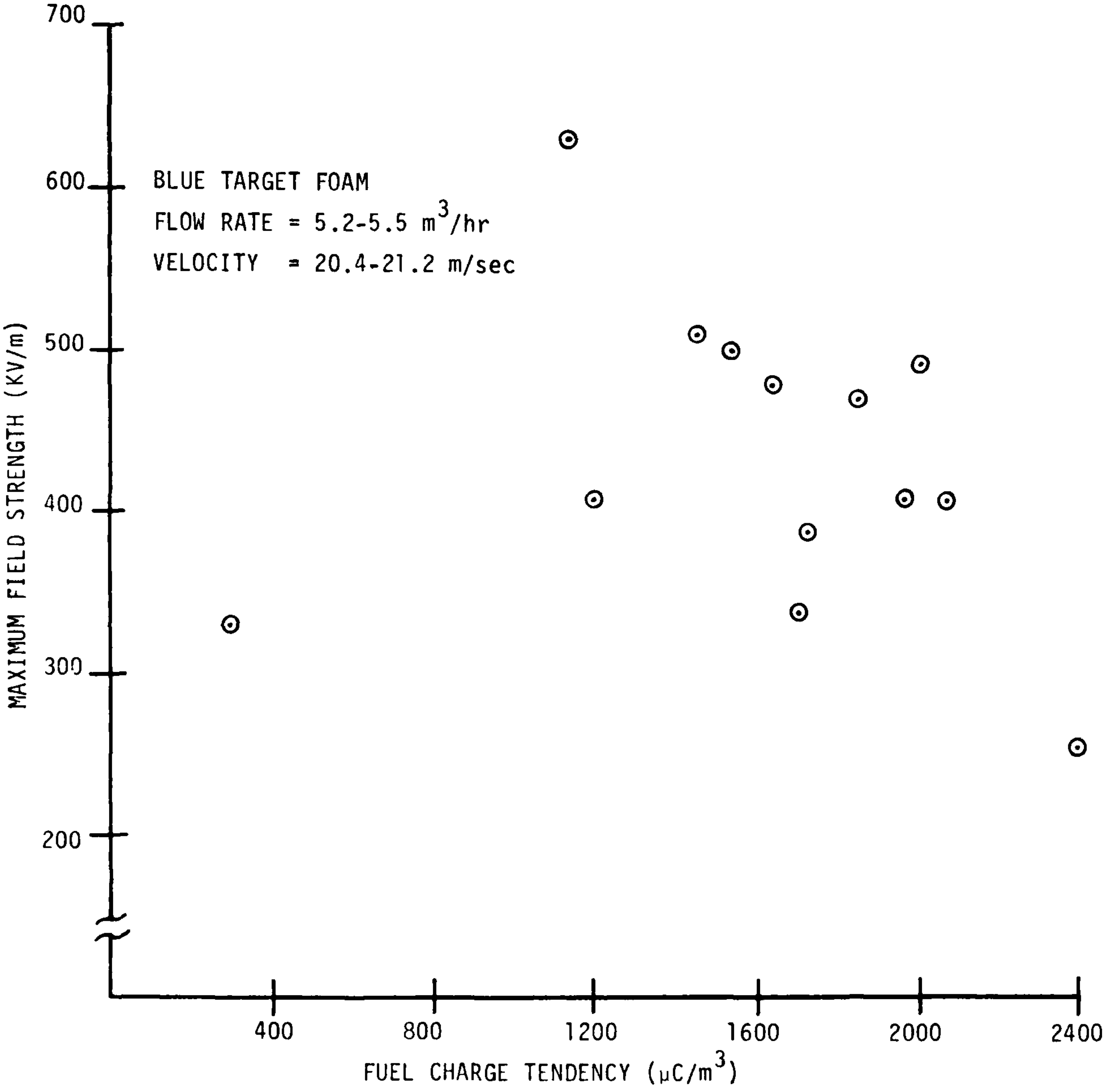

Figure 6. Maximum Field Strength Using .95 Cm Inlet vs. Charging Tendency of JP-4 Fuel

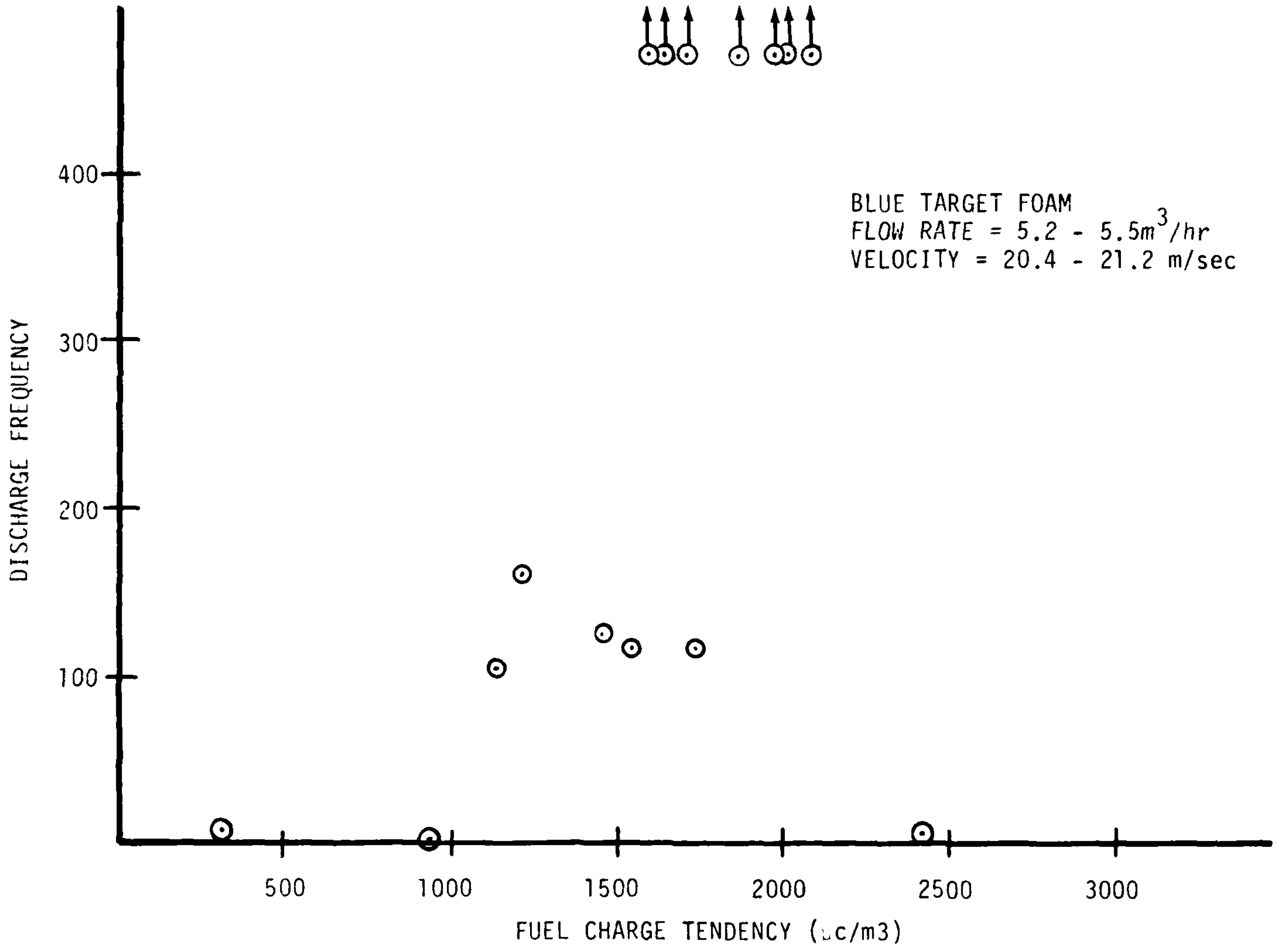

Figure 7. Discharge Activity Using 0.95 Cm Inlet vs. Charging Tendency of JP-4 Fuel

During fuel conductivity measurement testing, the charge generating tendency of the fuel, as defined earlier, was also measured. The data is shown in Table 3 and plotted in Figure 9. It was found that the charging tendency of the fuel increased by approximately six times (500 to 2800 $\mu C/m^3$). This indicated that ionizable substances were sorbed by the fuel from the foam. Monsanto Research Corporation was tasked with determining the specific substances that were being sorbed. Monsanto concluded (Appendix D) that the foam was absorbing substances (alkylphenols) from the fuel and that the fuel was extracting chemicals (the most significant being diethylhexal phthalate) from the light blue polyether (TYPE V) foam.

2. FUEL/FOAM IMPINGEMENT PHENOMENA

As was previously stated, the test data is limited in determining the effects of increasing charging tendency and fuel conductivity on charge generation and discharge frequency due to the everchanging factors involved (i.e., fuel and foam interaction). However, Figure 10 illustrates another fuel/foam interaction phenomena that was observed during baseline fuel flow testing. Note in this report, discharge frequency is defined as the number of spark discharges which were detected per test, and target foam number is defined as the number of tests a target foam was used. It was determined that as the number of fuel flow tests performed on a particular target foam section increased, the frequency of discharging decreased. Mills (Reference 9) also observed that the electrostatic activity was highest during new blue foam testing than during used blue foam testing. Upon analysis of used target foam sections, it was observed that the target foam sections experienced physical deterioration in terms of erosion of foam cell structure, foam color lightening around the fluid impingement area, and the breaking of foam cells. The amount of physical deterioration depended upon the number of times fuel flow impingement took place and the flow rate/velocity of the fluid stream.

Since it was known that physical deterioration of the foam was taking place and that a fuel/foam chemical interaction was occurring (Monsanto Report, Appendix D and Reference 9), two target foam sections (10 cm x 15 cm x 15 cm) were presoaked in JP-4 fuel for 24 and 28 hours (Tests 17 and 22), respectively. The target foam sections were then placed in the test tank to determine whether "aging" of the foam in JP-4 fuel would produce the chemical reaction and, thus, eliminate the electrostatic discharging observed. As can be seen in Appendix C, Tests 17 and 22,

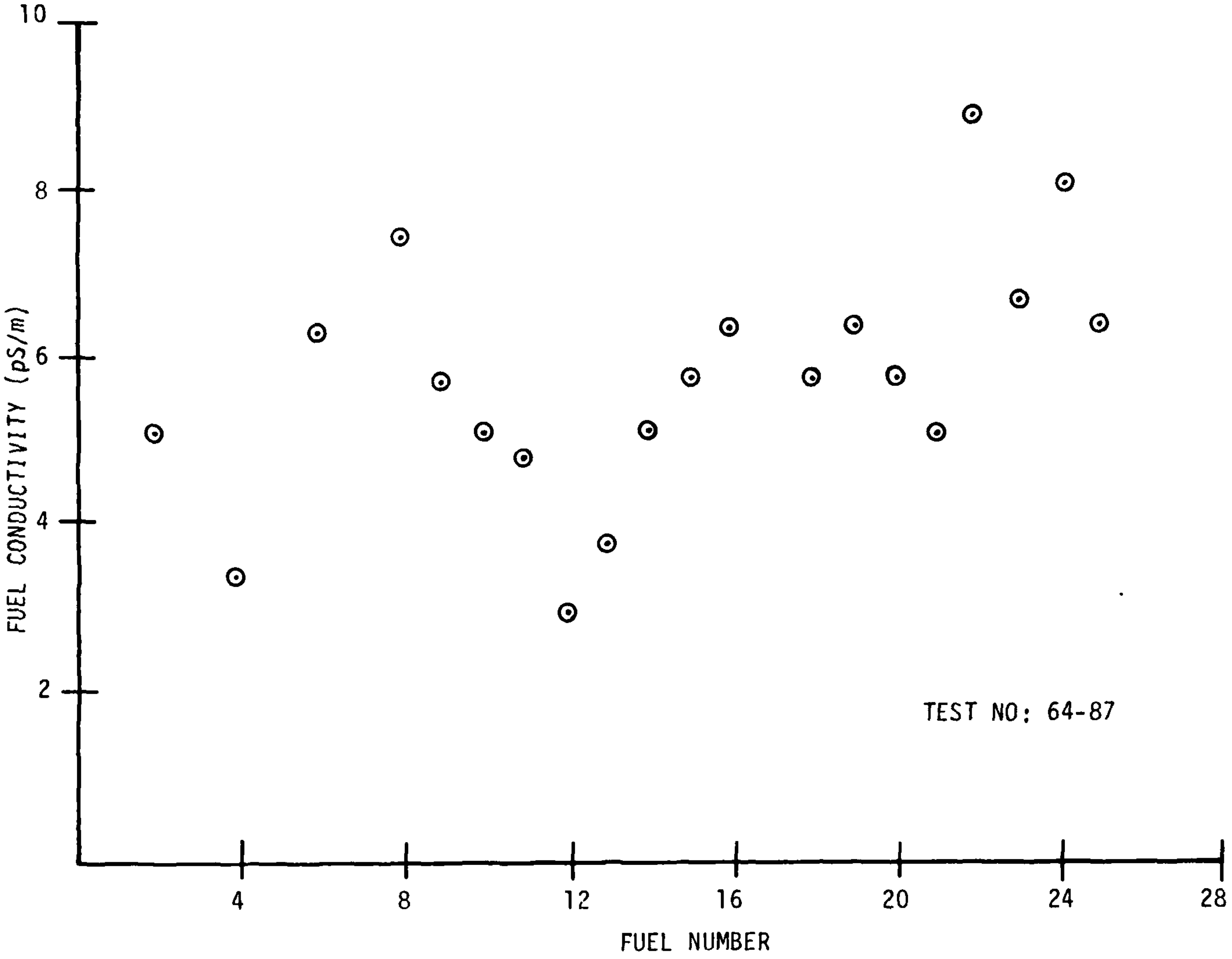

Figure 8. JP-4 Fuel Conductivity vs. Frequency of Fuel Use

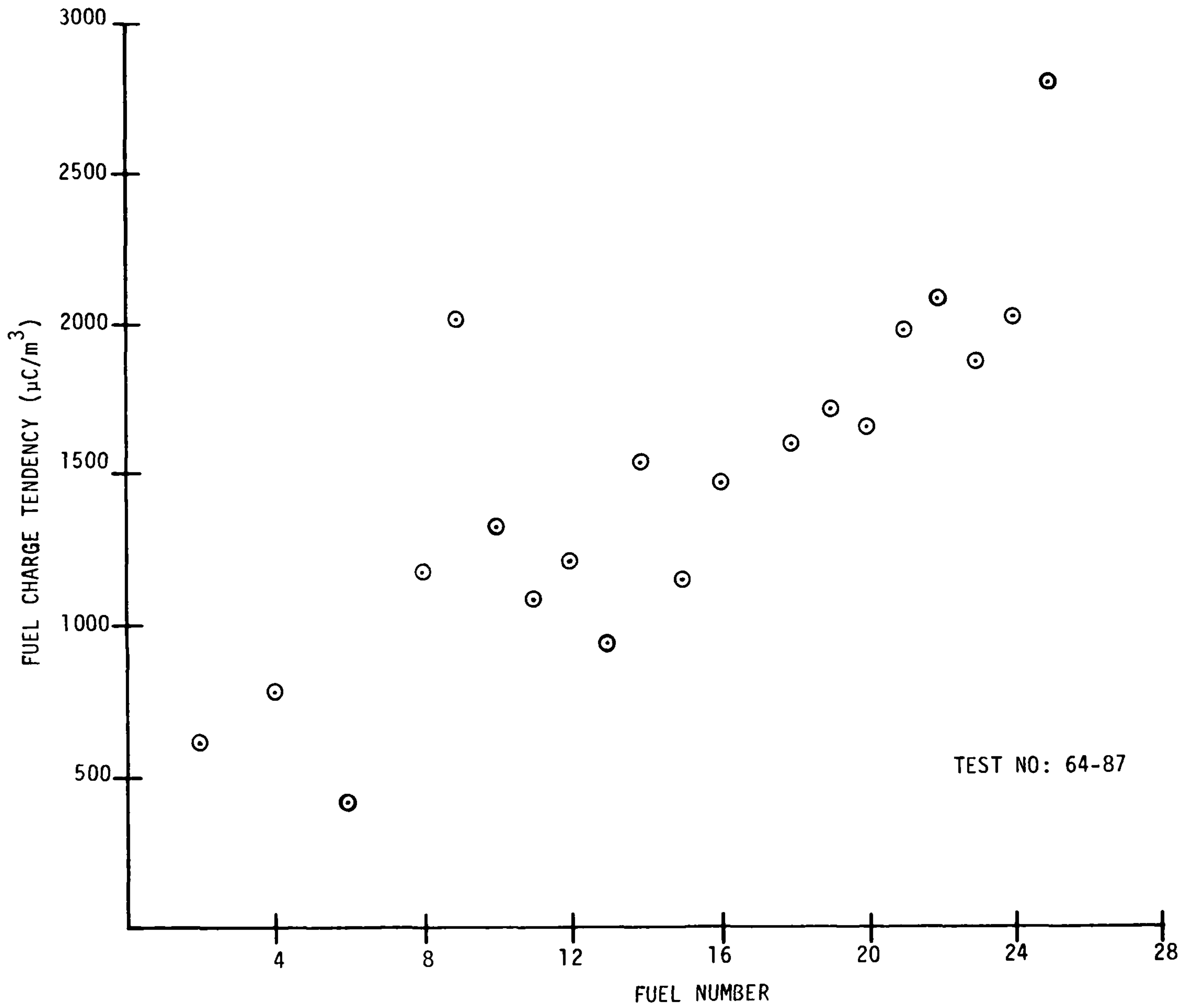

Figure 9. Charging Tendency of JP-4 Fuel vs. Frequency of Fuel Use

TABLE 3

EFFECTS OF FUEL USAGE ON CHARGING TENDENCY - CONDUCTIVITY

Test	Fuel	Fuel Temp(°C)	Fuel Conductivity (pS/m)	Charge Tendency (μC/m^3)
64	1		---	---
65	2	20	5.1	618
66	3		---	---
67	4	20	3.4	781
68	5		---	---
69	6	17	6.3	405
70	7		---	---
71	8	17	7.4	1170
72	9	17	5.7	2016
73	10	18	5.1	1310
74	11	13	4.9	1088
75	12	13	2.9	1209
76	13	12	3.7	942
77	14	14	5.1	1546
78	15	13	5.7	1148
79	16	11	6.3	1472
80	18	12	5.7	1599
81	19	13	6.3	1715
82	20	16	5.7	1649
83	21		5.1	1973
84	22	13	8.8	2083
85	23	13	6.6	1863
86	24	13	8.0	2017
87	25	13	6.3	2795

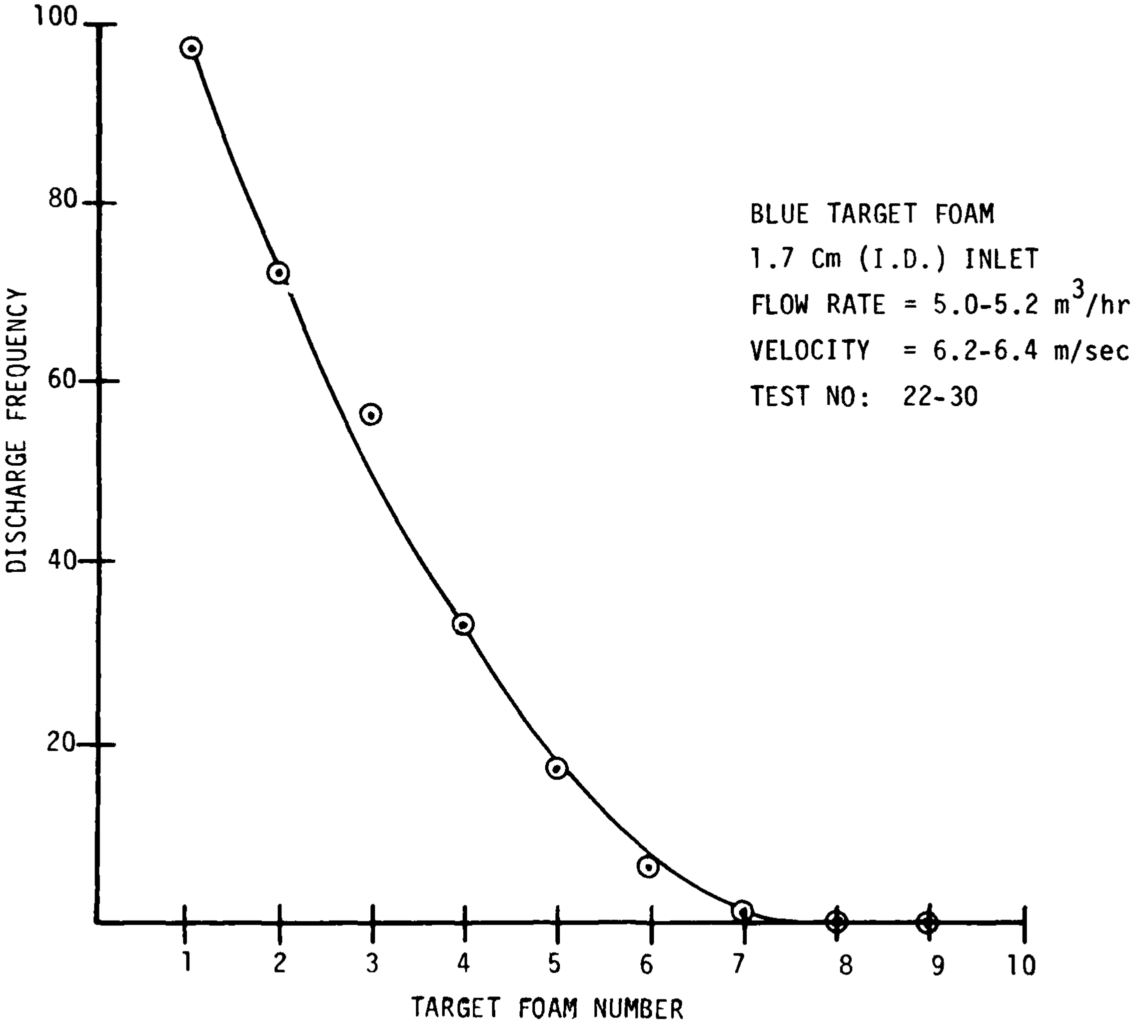

Figure 10. Discharge Frequency vs. Target Foam Number

both produce numerous discharges (73 and 97, respectively). The target foam section treated for 48 hours showed signs of physical deterioration (nine tests performed) where fuel impingement had taken place. The target foam section was then rotated 90 degrees after discharging had disappeared (Tests 29 and 30). After the target foam section was rotated, discharges were once again observed (Test 31); however, after repeating the test, no discharges were noted (Test 32).

Similar testing (Test 77) was performed; however, methanol was used as the "aging" fluid with no significant differences in the results. It is believed that a combination of the two factors (physical deterioration/chemical interaction) is involved in reducing the electrostatic discharge hazard, though the role of each factor in reducing discharging cannot be determined from the current test results.

3. DISCHARGE FREQUENCY AS A FUNCTION OF FIELD STRENGTH

The number of discharges occurring during fluid flow is known to be a function of charge accumulation and discharge gap distance (Reference 10). In the previous Results section data was reported in terms of the number of discharges which occurred during a particular test run (discharge frequency). Charge transfer measurements were made with an oscilloscope for a number of these discharges. Of the few measured, charge transfer levels as high as +90 nanocoulombs were observed. In addition, higher charge transfer levels were witnessed (both positive and negative polarity) with the electrometers. However, due to the slow frequency response associated with the electrometers, an accurate charge transfer measurement could not be made but a minimum value could be determined. Grenich and Tolle (Reference 11) have reported that charge transfer levels as low as +140 and -47 nanocoulombs have ignited hydrocarbon/air mixtures. This indicates that some of the charge transfer levels witnessed during this testing were of sufficient energy to ignite the fuel tank ullage area if the proper fuel/air mixture was present. However, as stated previously, all testing was performed in an inert environment to reduce testing turn-around time and to conserve polyurethane foam.

Figure 11 illustrates the dependence that the number of discharges which occur during a test has on charge accumulation. Although this figure shows wide data scatter, it was felt that a trend existed. This test data includes all the baseline JP-4 fuel testing without taking into account the number of times the fuel was used for testing or the number of times the target foam section was changed. Since these factors do influence both charge generation/accumulation and discharge occurrence/frequency (as shown earlier), it was felt that this may be the reason for the large data scatter. Data from a test series where the target foam section was unchanged clearly demonstrates this trend, as can be seen in Figure 12. In this test series, the discharge gap distance remained essentially constant since the target foam configuration was undisturbed. As expected, based on Figure 11, the number of discharges detected increased with increasing maximum field strength; and it again shows the relationship that with repeated testing with the same fuel and foam, the discharge frequency and field strength decreased (test series progressed from right to left in Figures 11 and 12). Figure 12 does not, however, illustrate the constant field strength value where discharge activity increases but the field strength measurement does not, but Figure 11 does. In Figure 11, the discharge frequency was extremely high (1000 discharges per test) for a number of tests whose field strength was above 300 KV/m. If little or no discharge activity was occurring, these measured field strengths would most likely be much higher.

The previous discussion assumes that discharging is taking place in the void space area around the inlet nozzle and target foam section since charge accumulation would be maximum in this location due to the localized fuel impingement. Due to the significant role that discharge gap distance has on the occurrence of discharging (Figure 11 vs. Figure 12), later test results will stress maximum field strength as the primary measurement variable since the effect of gap distance on field strength is believed to be less pronounced than it is for discharge occurrence/frequency. However, it must be kept in mind that for tests which experienced a high number of spark discharges, their measured field strengths may have been even higher in magnitude if no discharge activity had been present.

a. Fuel Flow Rate/Velocity Analysis

The effect of fuel flow velocity on charge separation and accumulation has been studied by many (References 12 and 13). The relationship obtained in this test program for maximum field strength vs. fuel flow velocity is shown in Figure 13. Two sets of data are provided in this figure. The effects of flow velocity on maximum field strength were obtained using the straight 1.7 cm (I.D.) diameter 304 stainless steel inlet tube and the 0.95 cm orificed 304 stainless steel inlet tube.

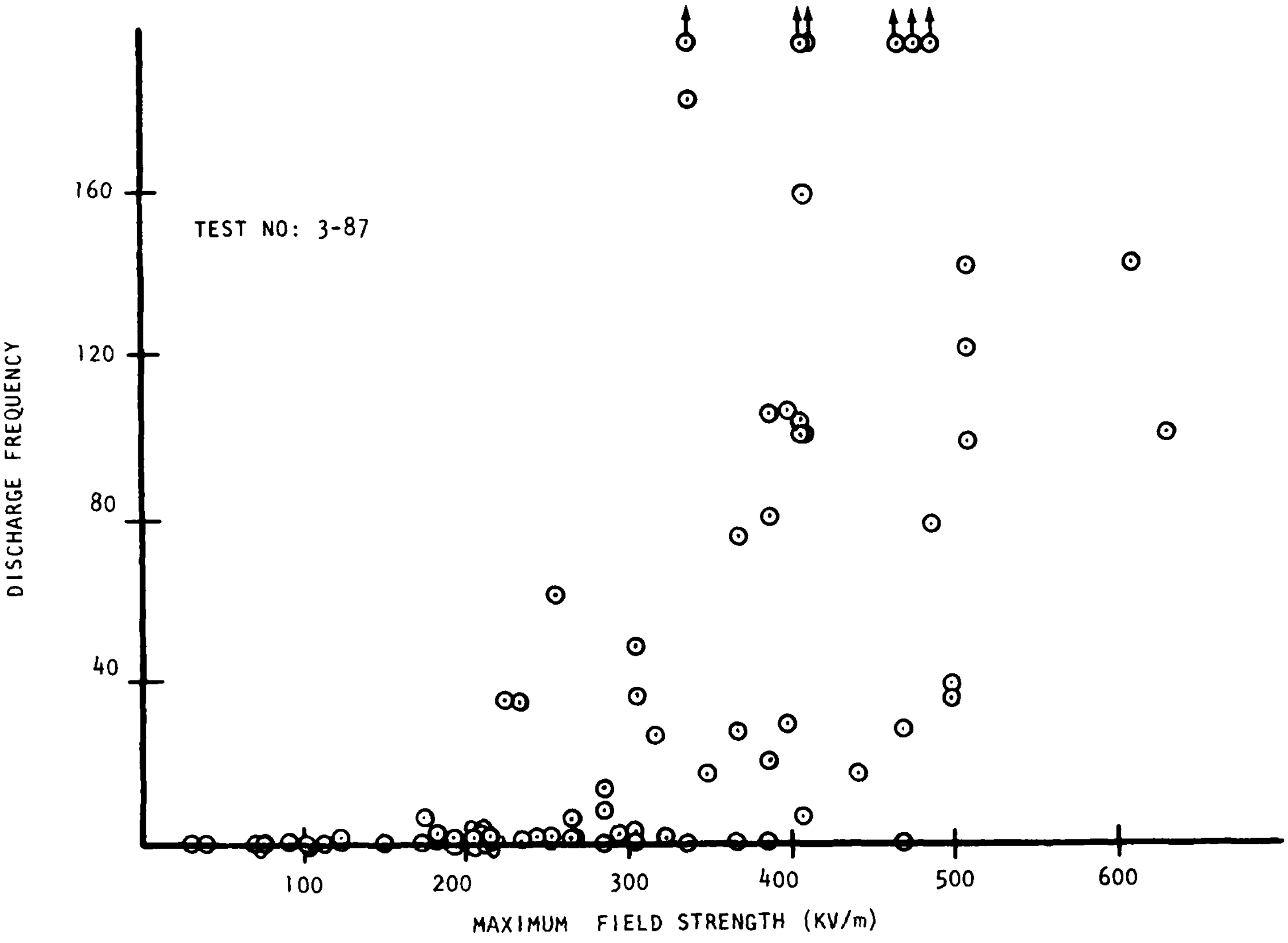

Figure 11. Discharge Frequency vs. Maximum Field Strength

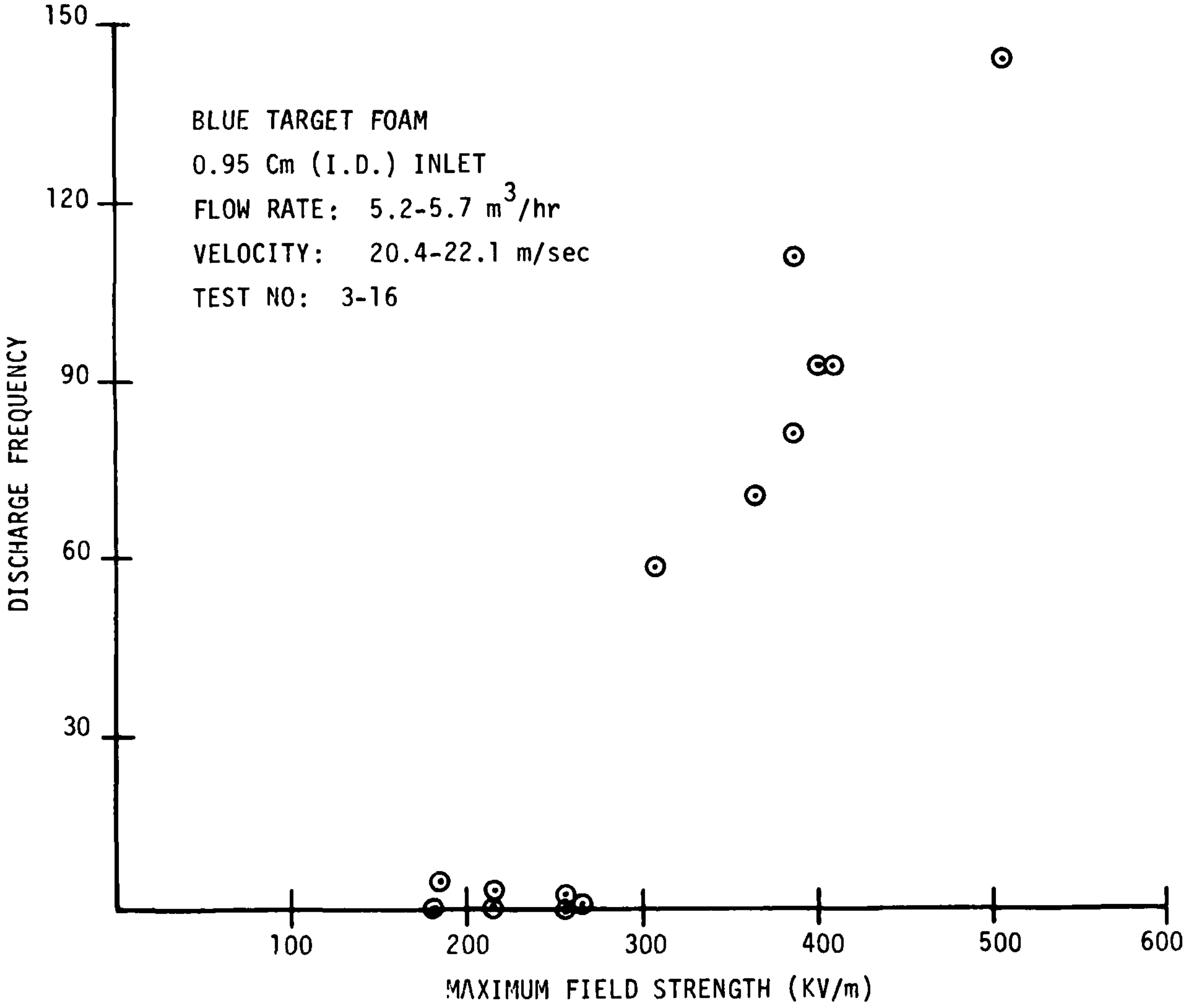

Figure 12. Discharge Frequency vs. Maximum Field Strength

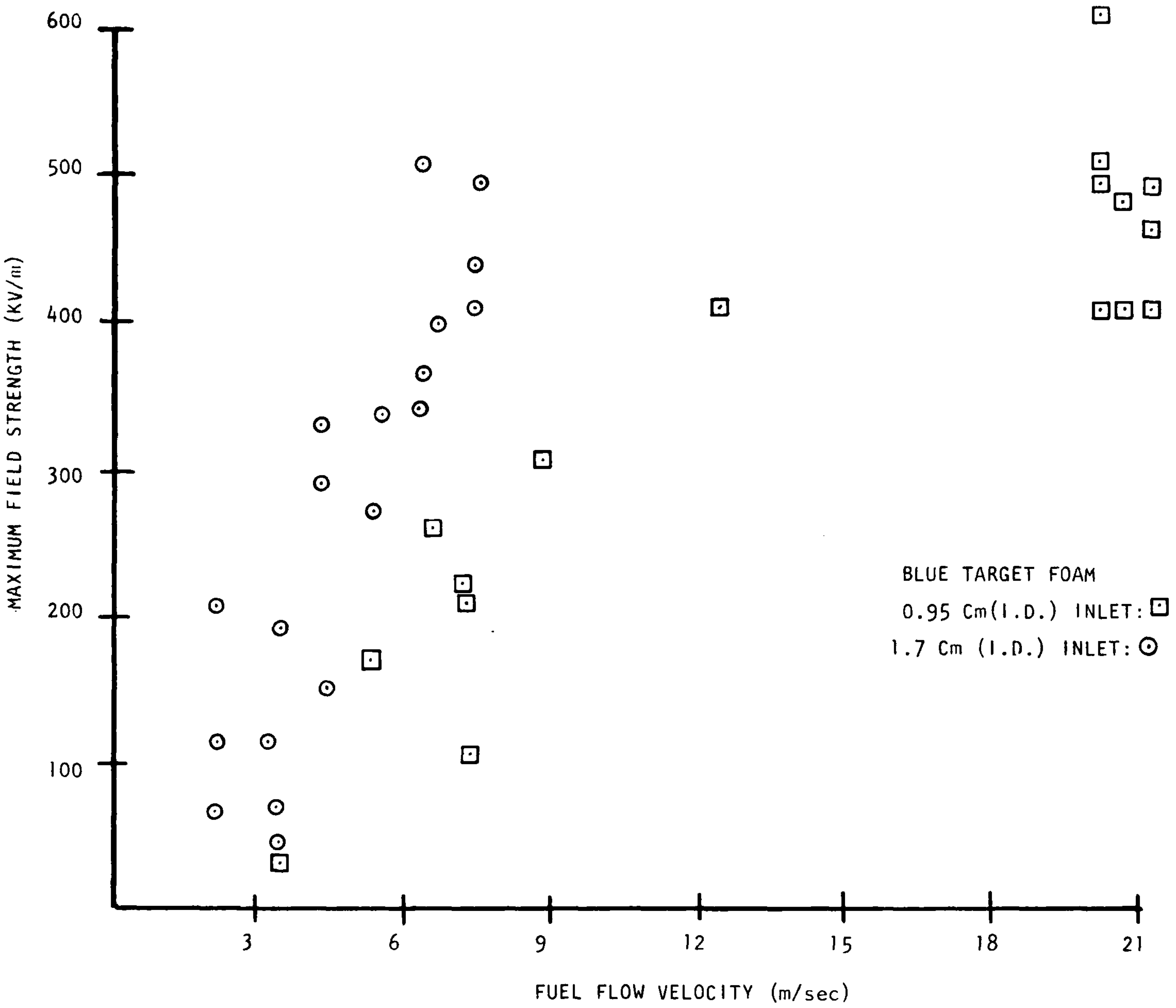

Figure 13. Maximum Field Strength vs. JP-4 Fuel Flow Velocity

As this figure illustrates, the maximum field strength increased when the fuel flow velocity increased; however, there is a distinct difference in the rate at which this occurred for the two inlets. For a given fuel flow velocity, the 1.7 cm inlet tube's maximum field strength was higher than the 0.95 cm inlet tube's maximum field strength (e.g., at 6 m/sec maximum field strengths were approximately 360 and 200 KV/m, respectively).

Variables such as fuel temperature and target foam section "aging" were controlled by a fuel refrigeration unit and by testing with new target foam sections in each test. The only significant variable in this section of testing was the diameter of the inlet tubes. This difference in inlet tube diameters directly affects the amount of foam surface area the fuel can impinge upon. By increasing the fuel-foam impingement area, the amount of charge separation increases. Since past electrostatic research efforts were mostly concerned with filter housing charge separation, the effect of surface area impingement was not considered a major variable due to the fact that the filter housing surface area is constant and totally flooded with fuel. However, in Figure 13 the maximum field strength plotted against the flow velocities of the 0.95 cm and 1.7 cm inlet tubes illustrate the significance of fuel impingement on foam surface area (proportional to inlet diameter). Figure 14 illustrates the effect of fuel flow rate on maximum field strength. It can be seen that the maximum field strength increased as the fuel flow rate increased; however, the two inlet tube's maximum field strength readings increased at different rates. For a given flow rate, the 0.95 cm inlet produced a higher maximum field strength than the 1.7 cm inlet tube. This is exactly opposite to Figure 13, but it must be kept in mind that the velocity is three times higher for the 0.95 cm inlet than for the 1.7 cm inlet tube. Therefore, taking both Figures 13 and 14 into consideration, one is left with the conclusion that the amount of charge separation that can take place is a function of both effective surface area (proportional to flow rate) and velocity.

b. Polyester Target Foam Testing

The last topic under JP-4 fuel baseline testing is the result of the red and orange target foam section testing (Tests 34 through 38, and 76). The test tank remained packed with light blue polyether foam (TYPE V); however, the light blue target foam sections were replaced with less resistive red (TYPE III) and orange

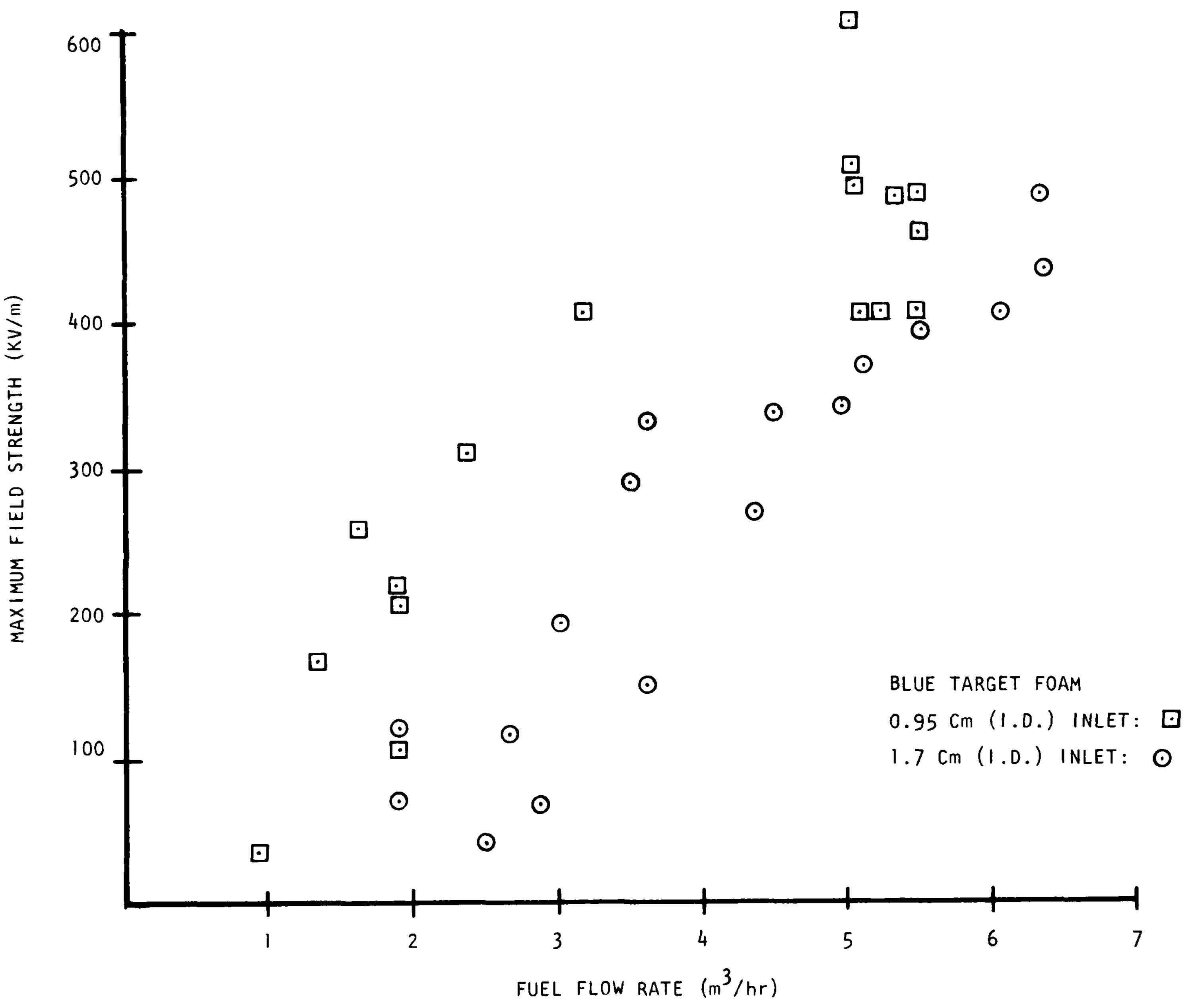

Figure 14. Maximum Field Strength vs. JP-4 Fuel Flow Rate

(TYPE I) target foam sections (Appendix A). During JP-4 fuel baseline testing, no discharging was observed with either red or orange target foam sections. Since testing was performed with 10 cm x 15 cm x 15 cm polyester target foam sections, it is not known whether this thickness would provide an aircraft fuel tank with a significant reduction in electrostatic activity due to the scaling factors involved and due to the different fuels' charge generating characteristics.

Using all the blue foam maximum field strength data which had target foam numbers less than or equal to three during baseline JP-4 fuel testing (Tests 3, 4, 5, 17, 39, 44, 47, 48, 75, 77, 78, 79, 81, 82, 83, 84, and 86), an average field strength of 438 KV/m was determined. These tests all had a flow rate of 5.35 ± 0.15 m^3/hr (23.5 ± 0.5 GPM) and a velocity of 20.8 ± 0.4 m/sec (68.3 ± 1.5 FPS). The red target foam's maximum measured field strengths under the same flow conditions (Tests 34, 35, 36, and 76) averaged a factor of approximately 1.6 less than the blue target foams' average. The orange target foam averaged a factor of 4.5 less than blue (Tests 37 and 38). As mentioned earlier, these field strength averages cannot be considered absolute since the field strength measurements associated with the blue foam testing may have been higher if no spark discharge activity was taken place.

Leonard and Affens (Reference 7) performed small scale charge generating tendency foam tests (not to be confused with the MST with Type 10 Facet paper) and found that the magnitude of charging tendency for the blue polyether foam was approximately six times greater than for the polyester foams. Mills (Reference 9) also reported that during their fuel flow testing, the blue foam charged anywhere from two to eighteen times higher than the red foam (depending on the fuel used). It is difficult to draw a direct comparison with Leonard and Affens' work since the foam surrounding the red and orange foams was blue polyether foam and discharge activity was taking place in several of the tests. However, it is interesting to note that the magnitudes are similar in regards to charge separation/accumulation.

4. SHELL ASA-3 CONDUCTIVITY ADDITIVE TESTING

With the completion of the baseline JP-4 fuel testing, the fuel's conductivity was gradually increased from approximately 6 to 160 picosiemens per meter (pS/m) using the Shell ASA-3 fuel conductivity improvement additive. Testing with the fuel conductivity additive was performed in conjunction with new light blue target foam sections (i.e., discharge gap most likely varied) and with the 0.95 cm and 1.7 cm inlet tubes. The gradual increase in the fuel's conductivity was expected to provide a decrease in the maximum field strength (and discharge frequency); however, as is shown in Figure 15, the maximum field strength initially increased. The maximum field strength reached its highest level of 660 KV/m at a fuel conductivity of 18.3 pS/m, whereas the baseline fuel tests (Tests 82 through 87) produced field strengths between 406 and 488 KV/m.

Once the fuel's conductivity increased above the 20 pS/m range, the field strength level began to decrease. At a fuel conductivity of 159.9 pS/m the maximum field strength had dropped to 10 KV/m with no indication of discharging. Dukek, et al (Reference 13) and Mills (Reference 9) also reported that at initial fuel conductivity levels above their baseline fuel conductivity, the discharge frequency increased; but with additional ASA-3, the frequency of discharging decreased.

From Figure 15 it can be seen that increasing the fuel's conductivity level above 20 pS/m will decrease the maximum field strength/discharge frequency. The conductivity level that is required to decrease the maximum field strength, thereby eliminating discharging, is dependent upon a number of factors. Comparing results of this program with other reported results (References 6, 9, 13, 14), one comes to the conclusion that the significant differences in the conductivity fuel additive requirement for elimination of discharge activity is highly dependent upon fuel tank/foam configuration, fuel ionizable impurities and additives, and fuel flow rate/velocity foam impingement phenomena. It must also be stated that a more hazardous condition could result if the fuel conductivity is at a level where the electrostatic charging hazard actually increases due to greater charge separation without a substantial increase in charge relaxation.

5. GULF-178 PRO-STATIC ADDITIVE TESTING

Testing of the Gulf-178 pro-static additive (Reference 4) was performed to determine the effect a severe charge generating JP-4 fuel would have on the maximum field strength/discharge frequency during refueling operations. Tests 103 through 129 (Appendix C) were conducted using the Gulf-178 additive. New light blue target foam sections and the 0.95 cm orificed inlet tube were used for all tests with the exception of Tests 125 and 126. These two tests substituted red and orange target foam sections for the blue sections. The Gulf-178 additive was injected in increments of approximately 15 cc per 0.38 m^3 of JP-4 fuel.

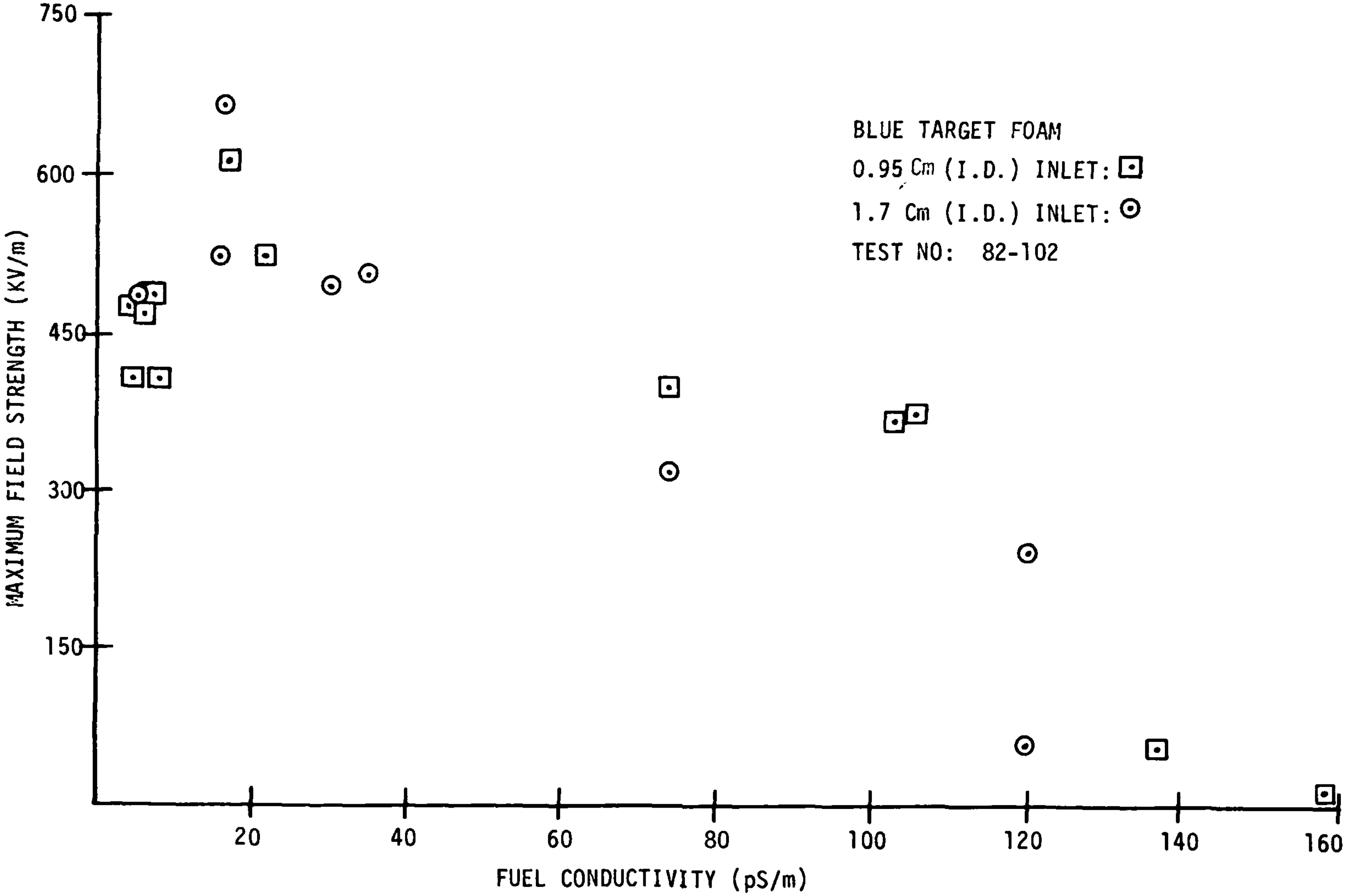

Figure 15. Maximum Field Strength vs. JP-4 Fuel Conductivity Level

From Figure 16, it can be seen that the maximum field strength gradually changed from a positive to a negative polarity with increasing Gulf-178 additive concentrations. The plot shows that the maximum field strength increased to approximately -340 KV/m for a Gulf-178 concentration of about 360 parts per million (ppm). The maximum field strength remained relatively constant (approximately -300 KV/m) between Gulf-178 concentrations of 300 and 1200 ppm. Reasons for this phenomena are not known at this time.

When the Gulf-178 additive concentration was increased to 1585 parts per million, the maximum field strength increased to -1016 KV/m (Tests 127 through 129). These maximum field strengths were the highest recorded during the entire program. At this concentration (1585 ppm), only small changes in maximum measured field strengths (KV/m) were observed when substituting the red target foam (-966 KV/m; Test 125) and the orange target foam (-812 KV/m; Test 126) for the blue target foam section. During baseline fuel/foam testing (Tests 1 through 87), the difference between blue polyether and the polyester foams, in terms of maximum field strength averages, was significant (e.g., blue: +438 KV/m; red: +274 KV/m; and orange: +97 KV/m). However, with Gulf-178 additive fuel, the difference in measured field strength is minimal. Therefore, it appears that the Gulf-178 additive plays a greater role in the charge separation phenomenon while the foams (polyether vs. polyester) play a less significant role. Of course this could also be attributed to the subsequent discharge activity hindering the respective field strengths for each of the three foam types so that little difference could be detected. (Note: the discharge activity did slightly decrease for the polyester foams: blue foam had 594 discharges, red had 560 discharges, and orange foam had 202 discharges.)

6. SHELL ASA-3 AND GULF-178 ADDITIVE TESTING

The last section of testing concerned the effect of fuel conductivity on the maximum field strength (discharge frequency) of a highly active JP-4 fuel. Testing was conducted with the 0.95 cm orificed inlet tube, new light blue target foam sections, and 1585 parts per million Gulf-178 additive fuel. The fuel was doped to this additive level since this was the highest level of pro-static additive concentration tested previously (see Section III, Part 3). This concentration also provided the highest maximum field strengths witnessed during the entire test program and produced discharging with polyester target foam sections (orange and red).

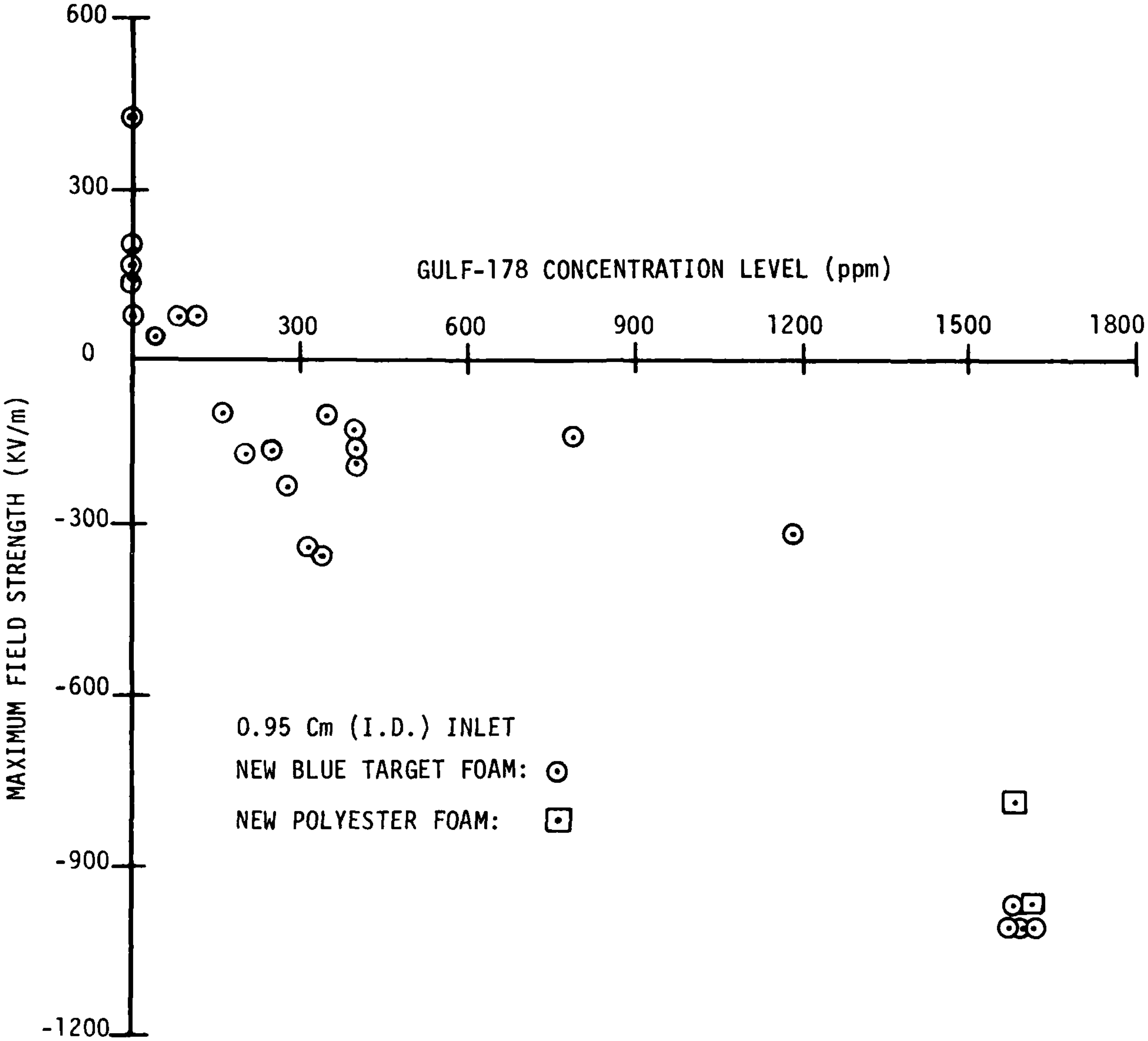

Figure 16. Maximum Field Strength vs. Gulf-178 Pro-Static Concentration Level

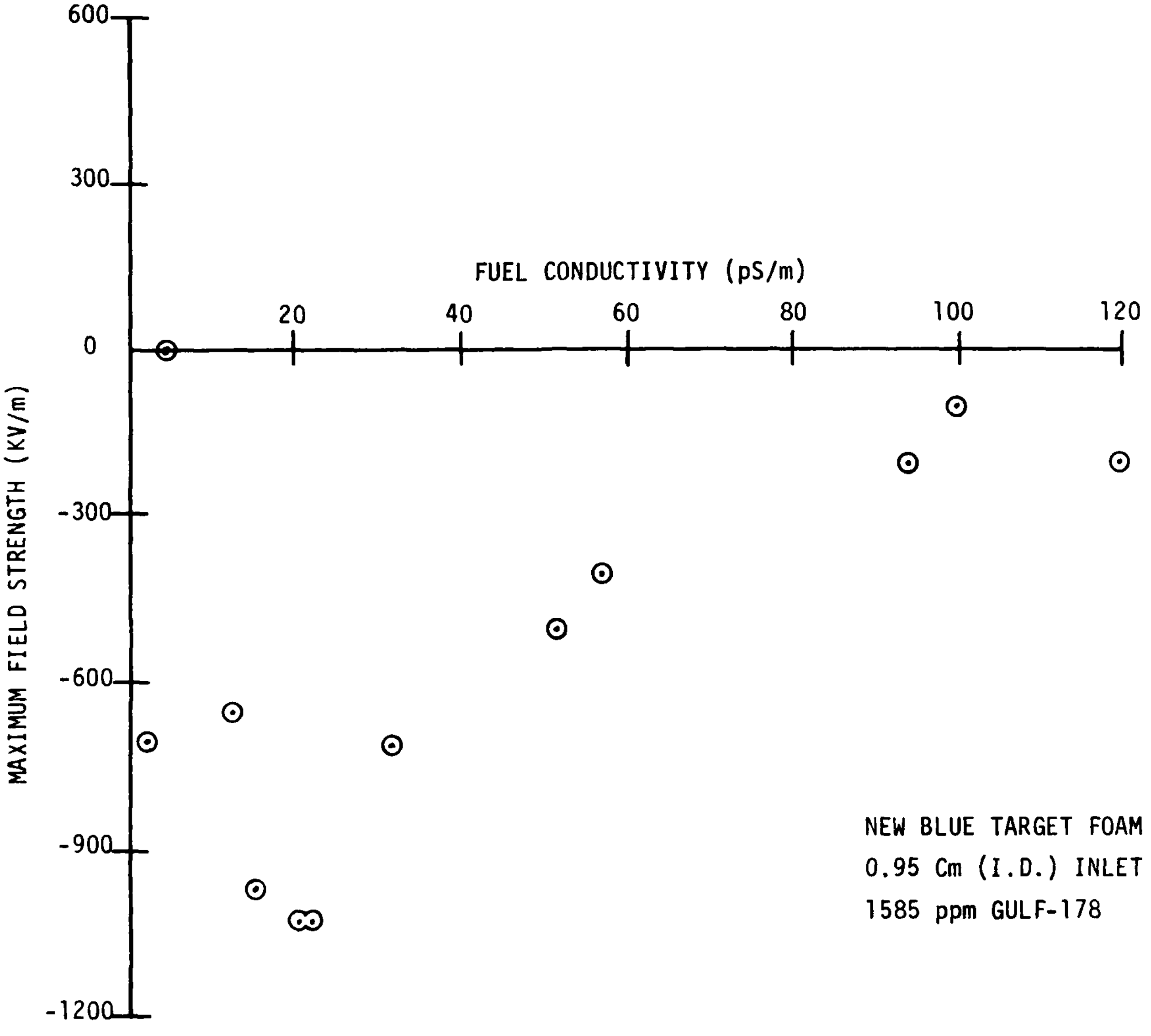

Figure 17. Maximum Field Strength vs. Conductivity of Pro-Static JP-4 Fuel

As is shown in Figure 17, the maximum field strength initially increased in magnitude to approximately -1000 KV/m at a fuel conductivity of approximately 20 pS/m. This initial increase in field strength also occurred at this conductivity level with baseline JP-4 when ASA-3 conductivity additive was used (Figure 15). The maximum field strengths were opposite in polarity as was the case during baseline Gulf-178 additive testing (Figure 16). Once the fuel's conductivity was increased beyond the 20 pS/m point, the maximum field strength magnitudes gradually decreased to the 100-200 KV/m range.

There appears to be no significant difference in the conductivity levels at which maximum field strengths (discharge frequency) decreased to a "safe" level (100 KV/m for this specific test apparatus; see Figure 11) for both the baseline fuel and the pro-static fuel when ASA-3 conductivity improvement additive was used. One would suspect that the fuel conductivity level requirement for reducing/eliminating discharging would be much higher when an electrostatically active fuel (-1000 KV/m) was encountered. However, this was not the case for this particular combination of test fuel and Gulf-178 additive. Further testing of other fuels would have to be performed to obtain a better understanding of the problem. During this phase of the program, however, time requirements limited the scope of test parameters which could be studied.

SECTION IV

CONCLUSIONS

The emphasis of this electrostatic program was to simulate, on a dynamic basis, the static electricity fire hazard that was taking place during aircraft ground refueling operations. Once the static electricity problem was simulated, an understanding of its causes could be studied, and solutions obtained. It must be pointed out that although an attempt to realistically simulate aircraft refueling operations was made in this program, the data should not be extrapolated to actual aircraft environments due to the scaling factors involved (i.e., inlet design/location, foam type/pore size, fuel flow rate/velocity, tank geometry/plumbing, fuel charging characteristics, fuel spray patterns, etc.).

Since data scatter was a major problem, trends were very important in establishing a basic understanding of the factors that govern electrostatic discharge activity. The following conclusions are based on the experimental results provided in the body and appendices of this report.

- It could not be shown in the Results and Discussion Section that the Exxon Mini-Static Test Procedure was useful in correlating the charge generating tendency (TYPE 10 paper) of JP-4 fuel with charge accumulation levels produced during foam packed fuel tank testing. Due to this unresolved issue, the Exxon Mini-Static test method should not be used in the future to characterize the electrostatic potential of a hydrocarbon fuel when analyzing the susceptibility of a foam packed fuel tank to discharging hazards.

- The light blue polyurethane foam's (TYPE V) volume resistivity was in the 10^{15} ohm-cm range, the red (TYPE III) and yellow (TYPE II) were 10^{14} ohm-cm, and the orange (TYPE I) was 10^{13} ohm-cm. Since blue foam is at least one order of magnitude greater than the red and orange foams, it can be concluded that the blue polyurethane foam will have a lower charge relaxation rate. This lower charge relaxation rate will result in a higher charge accumulation level (assuming equal or greater charge generation rates).

- As was expected, based on the preceding conclusion, the light blue polyurethane foam (TYPE V) produced the highest maximum field strengths, approximately 4.5 times higher than the orange (TYPE I) and 1.6 times higher than the red (TYPE III) foams. Therefore, the susceptibility of an aircraft to an electrostatically initiated refueling fire incident will be greater with fuel tanks packed with blue polyurethane foam if measures are not taken to decrease the higher charge accumulation levels.

- It was determined that electrostatic spark discharging was highly dependent upon fuel flow velocity, as well as flow rate. Flow rate was found to be important in regards to the amount of foam surface area that was impinged upon by the fuel. Since both flow rate and velocity are coupled for a particular inlet, the importance that each contributes to the charge generation process is difficult to obtain. One must take into account both flow rate (effective area) and velocity when analyzing the susceptibility of an aircraft fuel system to electrostatic discharging. Furthermore, a "safe" velocity can never be determined without taking into account a fuel's charging tendency in conjunction with foam and the flow pattern (effective area) involved.

- During repeated light blue polyurethane fuel-foam impingement testing, it was observed that electrostatic discharging ceased due to either a fuel-foam chemical interaction, a foam deterioration process, or a combination of both. Though electrostatic discharging did cease after a number of tests, determining the number of actual aircraft refuelings that must take place to eliminate electrostatic discharging for particular fuel tank configurations cannot be estimated since the effects of scaling factors and the nature of the process are not known.

- Eliminating hazardous electrostatic spark discharging during aircraft ground refueling operations can be accomplished with the Shell ASA-3 fuel conductivity improvement additive. It must be pointed out, however, that the required fuel conductivity level is dependent upon scaling factors and the charge generating characteristics of the fuel. For the two fuels tested under this program (baseline JP-4 and the pro-static Gulf-178 additive JP-4 fuel), there was little difference in the fuel conductivity levels required to minimize electrostatic activities. This result, however, is only applicable to fuels which are made pro-static by adding Gulf-178 to the fuel. It may not apply to fuels whose pro-static properties are caused by trace contaminants and ionizable impurities in the fuel. Therefore, it may take an impractically high level of conductivity improvement additive in a particular fuel to minimize electrostatic activities for certain fuel system and blue foam configurations.

SECTION V

RECOMMENDATIONS

It has become apparent, through this program and others, that additional work is required to increase the Air Force's understanding and margin of safety in the complex field of static electricity. The following is additional work that needs to be investigated:

- Improved Measurement Techniques

  Due to the lack of appropriate techniques for measuring an unknown distribution of charges accumulated on foam materials, only relative trends could be produced under this test effort. Therefore, improved measurement techniques must be developed before a quantitative level of hazard associated with electrostatic charge generation during fueling operations can be determined.

- Inlet Nozzle Design

  The results of many programs have shown that inlet nozzle design is very important in reducing electrostatic discharge activity. Many (References 6, 9, 13, 14) have tested simple straight tubes and piccolo (multiple holes in tube to reduce fuel velocity and intense localized charging) inlets; however, the most common inlet (F-4, F-15, C-130, etc.) in U.S. Air Force aircraft is the "shower-head" (distributes fuel in the same manner as a bathroom shower) inlet. This "shower-head" inlet should be analyzed along with new innovative inlets which will minimize high velocity fuel-foam impingement under operational flow conditions and varying tank geometries.

- Small Scale Test Apparatus

  The Exxon Mini-Static Test Apparatus could not be used to identify a fuel's susceptibility to produce electrostatic spark discharging during a refueling operation into an aircraft fuel tank packed with polyurethane foam. It is recommended that a test method be developed and correlated to a full scale refueling operation. The test method can be successfully demonstrated only if improved measurement techniques are available which can quantitatively discriminate (on a full scale basis) the electrostatic hazards associated with various jet fuels in conjunction with foam materials.

- Polyurethane Foam Conductivity and Additives

The foam has been found to be a major factor in the charge separation/accumulation process due to its open pore configuration, chemical additives, and volume resistivity. Therefore, additional work should be focused on reducing the volume resistivity of the polyurethane foams and on determining what specific blue foam additives are contributing to the increased charge generation-accumulation levels observed.

- Fuel Flow Rate Vs. Velocity

An attempt to determine the effect of flow rate vs. velocity on the electrostatic charge separation process should be initiated. This program has identified flow rate as being a major contributor to the charge separation process; however, the degree to which flow rate (or area of the foam affected) is a factor compared to velocity is not known.

REFERENCES

1. Military Specification, Baffle and Inerting Material, Aircraft Fuel Tank, Mil-B-83054B (USAF), May 1978.
2. J. A. Carruthers and K. J. Wigley, "Estimation of Electrostatic Potentials, Fields, and Energies in a Rectangular Metal Tank Containing Charged Fuel," Institute of Petroleum Journal, Vol. 48 (1962), pp. 180-195.
3. D. A. Young, Mini-Static Test Procedure, Linden N.J.: Exxon Research and Engineering Company, June 1972.
4. J. T. Leonard and H. F. Bogardus, Pro-Static Agents in Jet Fuels, Washington DC: Naval Research Laboratory, NRL Report 8021, August 16, 1976.
5. H. Strawson and A. Lewis, Electrostatic Charging in the Handling of Aviation Fuels, Shell Research Limited, August 1971.
6. P. W. Kirklin, Factors Affecting Electrostatic Hazards, Mobil Research and Development Corporation, Technical Report AFAPL-TR-78-89, December 1978.
7. J. T. Leonard and W. A. Affens, Electrostatic Charging of JP-4 Fuel on Polyurethane Foam, Naval Research Laboratory, March 3, 1978.
8. Standard Method of Test for D-C Electrical Conductivity of Hydrocarbon Fuels, ASTM D3114-72, Vol. 25, 1974.
9. J. S. Mills, Electrostatic Charging in Reticulated Foams, Shell Research Limited, Technical Report AFWAL-TR-81-2015, March 1981.
10. B. Lewis and G. von Elbe, Combustion, Flames, and Explosions of Gases, New York: Academic Press, Inc., 1961.
11. A. F. Grenich, F. F. Tolle, Electrostatic Safety with Explosion Suppressant Foam, Boeing Military Airplane Company, Technical Report AFWAL-TR-83-2015, March 1983.
12. Electrostatic Charging Characteristics of Jet Fuel Filtration Equipment, Coordinating Research Council, Inc., CRC Report No. 458, April 1973.
13. W. G. Dukek, J. M. Ferraro, and W. F. Taylor, Static Electricity Hazards in Aircraft Fuel Systems, Exxon Research and Engineering Company, Technical Report AFAPL-TR-78-56, August 1978.
14. D. Dantuono and E. Radgowski, Investigation of Electrostatic Discharge in A-10 Fuel Tanks During Refueling, Fairchild Republic Company, GT160R0164, March 27, 1978.
15. Standard Methods of Test for D-C Resistance or Conductance of Insulating Materials, ASTM D257.

REFERENCES (Continued)

16. A Survey of Electrical Conductivity and Charging Tendency Characteristics of Aircraft Turbine Fuels, Coordinating Research Council, Inc., CRC Report No. 478, April 1975.

17. Dr. Leo Parts, Research and Investigation of the Flammability of Aircraft Fuels and Related Materials, Monsanto Research Corporation, Progress Report Number 78-4, January 1978.

18. W. Allen, Proceedings of Mini-Symposium on Static Electricity Hazards During Aircraft Fueling, Aeronautical Systems Division, November 18, 1977.

APPENDIX A

DC RESISTANCE OF RETICULATED POLYURETHANE FOAMS (Reference 15)

Objective

The primary objective for characterizing the resistive qualities of the various polyurethane foams was to determine if the foam's conductive properties were contributing to the aircraft electrostatic refueling problem. The electrical properties of fine pore light blue foam (TYPE V), red foam (TYPE III), yellow foam (TYPE II), and orange foam (TYPE I) were determined using two different test methods. The first method measured the charge relaxation as a function of time (i.e., foam's charge decay time constant) for various foam thicknesses, while the second testing method consisted of measuring the volume resistivity of the foams (ASTM D257) under fuel wetted and dry conditions.

Test Method

Charge Relaxation Time Method Indicating Various Resistivities of Polyurethane Foams

The apparatus for the test consisted of a field strength meter, a 0-30,000 volt DC power supply, an electrostatic voltmeter, a Teflon® isolation base, and a metal plate used to uniformly charge the foams. These components were installed as shown in Figure A.1. The test method used does not attempt to provide absolute results concerning the time constants of the foams since the variables that govern charge relaxation rate of the foams were not adequately controlled (e.g., relative humidity and temperature). The quality of testing was also limited due to program time constraints, and the test apparatus repeatability was not determined for the same reason. The test method was used to obtain a relative ranking of the foams in regards to their charge relaxation rates.

The field strength measuring head was located one centimeter above the foam surfaces. The test voltages ranged from 10.2 - 10.4 kilovolts (KV). Four different foam samples were tested: light blue, red, yellow, and orange. In addition, three foam thicknesses were studied: 2.5 cm, 10 cm, and 30.5 cm (1 inch, 4 inches, and 12 inches).

After applying a voltage to the isolated stainless steel plate, a timer was triggered. In this manner the amount of time for the charge to travel from the

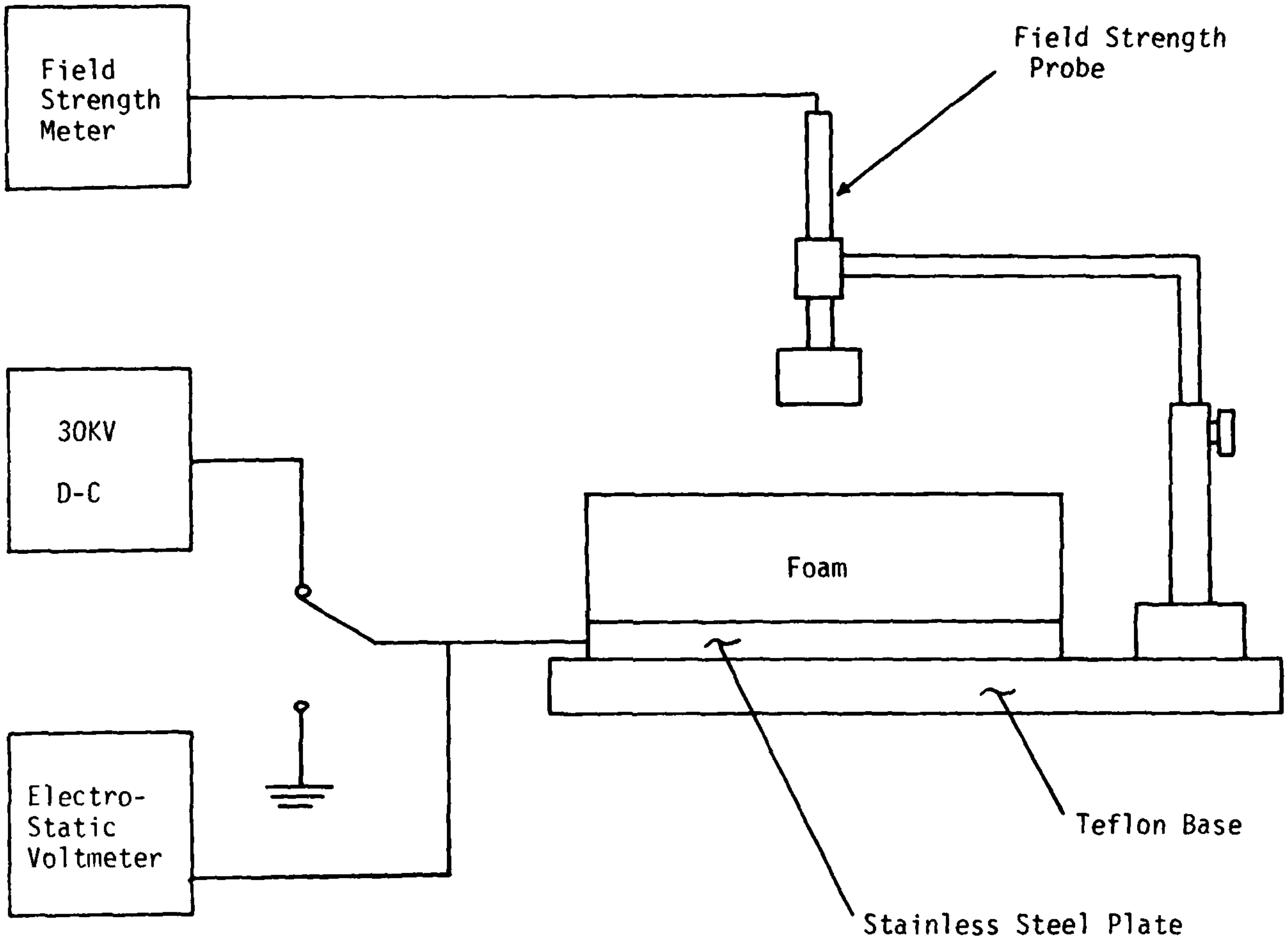

Figure A.1. Polyurethane Foam Charge Relaxation Time Constant Measuring Apparatus bottom of the foam to the top could be monitored. This is referred to as the charging time of the foam. Note that the charge at the top of the foam being monitored by the field strength meter will never read 100 percent of the applied voltage due to losses to air. After the top of the foam had reached its steady-state maximum voltage, the DC power supply was shut off and the stainless steel plate grounded. This procedure permitted the relaxation times of the foams to be studied also. The approach was to analyze and compare the foam samples' exponential decay curves and their resultant charge decay time constants.

Direct Measurement of Polyurethane Foam Resistivities

The volume resistivity of the foams was measured in accordance with the ASTM D257 standard as previously stated. A schematic of the test apparatus and the geometry of the electrodes is shown in Figure A.2. The electrodes consisted of the base stainless steel plate where voltage was applied, the center stainless steel plate which was connected in series with a resistor of known value and the outer stainless steel ring which served as a guard to allow a more true conductance of charge through the foam by minimizing the electrode edge electric field effects. The surface area and weight of the center plate and the surrounding ring were made equal to obtain equal fringing effects on the foam. Various applied voltages were used during the testing, and the value of the known resistor varied depending on the foam type being tested. Typically, the value of the resistor was approximately 100 times less than the resistance of the foam being tested (which was roughly determined by direct measurement). This allowed most of the voltage drop to occur through the foams, thereby, allowing the foams to control the amount of current in the circuit. The additional voltage drop through the known resistor could then be monitored on an electrometer. With this measurement plus the dimensions of the foam samples and the electrodes, the resistivity of the material could be calculated. The following formula for calculating the average volume resistivity of dielectric material is shown below. This formula is also provided in ASTM D257.

$$\rho_V = {}^{A}/_{t} \, Rv$$

where

$$A = \pi/4 \; (D = Bg)^2$$

$$= \pi/4 \quad D = g - \frac{4t}{\pi} \ln \cosh \frac{\pi g}{4t}$$

and

$R_V \quad (\frac{V}{V_s} \quad 1)R_s$ by using voltage divider technique

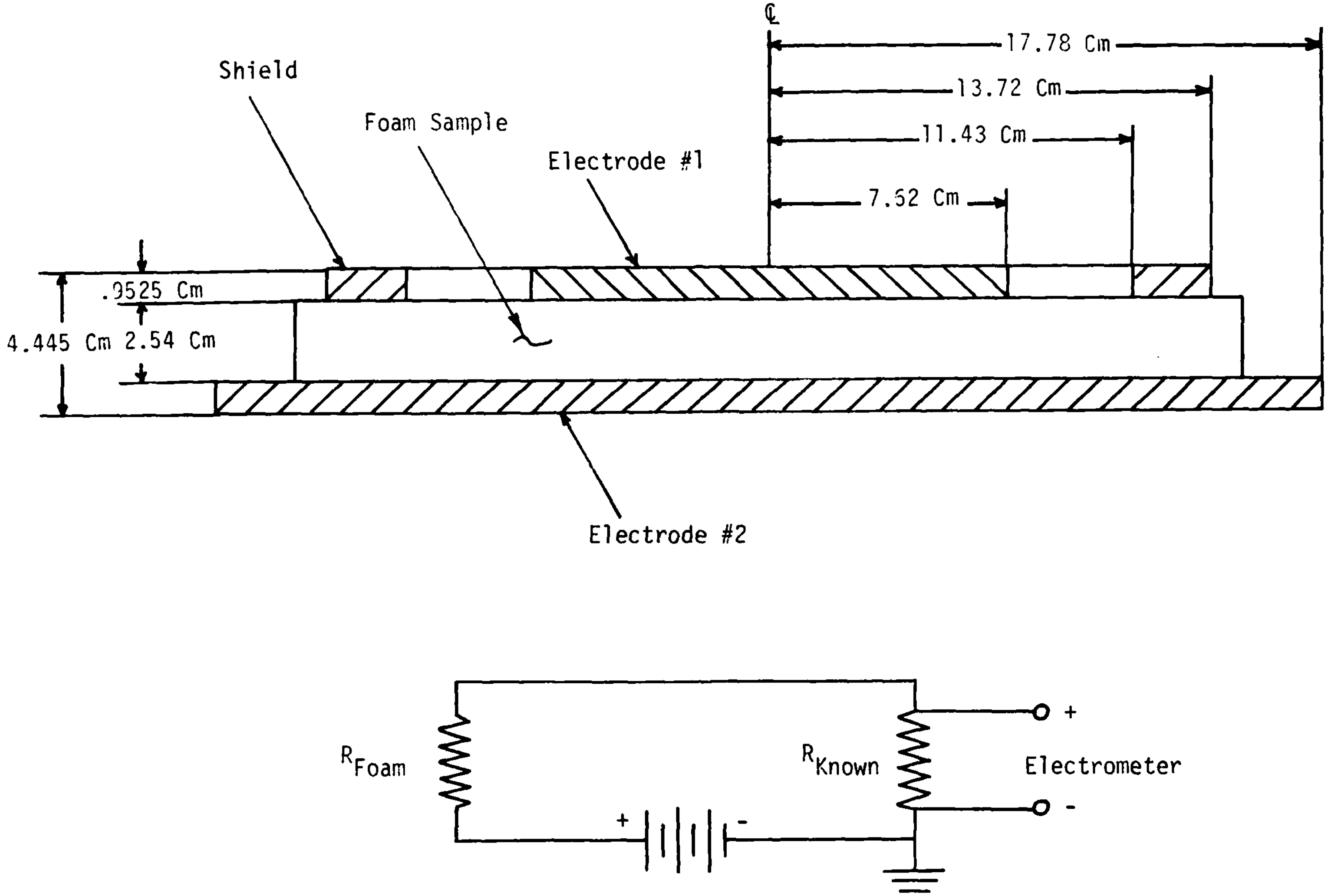

Figure A.2. Dimensional and Electrical Diagrams for Measuring Volume Resistivity of Polyurethane Foams with

ρ_v = volume resistivity (Ω - cm)

A = effective area of the measuring electrode for the circular electrodes

D = diameter of center electrode (cm)

g = gap distance between center electrode and outer ring guard (cm)

Bg = added distance due to fringing of the material with B equal to the fraction of the gap width which must be added to the diameter of the circular electrodes (cm)

t = average thickness of specimen (cm)

R_v = measured volume resistance of material (Ω)

R_s = resistance of known resistor (Ω) - typically $\sim{}^{1}/100\ R_v$

V = applied voltage (volts)

V_s = measured voltage across known resistor, R_s (volts)

Substituting all the values from Figure 1 into the above equations yields:

$$\rho_v = 232.08\left(\frac{R_s}{t}\right)\left(\frac{V}{V_s} - 1\right)$$

Results and Discussion

Analysis of the data is provided below. Once again, it should be noted that only trends for the foams' conductive properties could be determined since variances in the temperature and humidity from day to day impacted the repeatability of testing. This repeatability problem was observed even after baking the foams at a temperature of 60°C for 24 hours and nitrogen-purging the samples during testing. Though a problem with repeatability was observed, definite trends in regard to the relative conductance each foam displayed versus another foam was clear. This testing series was not intended to be exhaustive, but instead, to yield qualitative results needed to aid in the analysis of the charge accumulation/static discharge phenomena occurring within Air Force aircraft fuel tanks containing foam. It is believed that data repeatability could be improved if an environmental chamber is used in the future to determine the foams' volume resistivity and charge decay time constants. The following is a discussion of the data generated.

1. The typical behavioral effects of foam thicknesses vs. charging time is shown in Figure A.3. As expected, the thicker the foam sample, the greater the resistance is from the bottom of the foam to the top; therefore, the longer it takes the charge to migrate from bottom to top. This effect was clearly present with all the foam samples.

2. Figure A.4 illustrates various foam charging times under similar conditions. As can be seen, the blue foam required a much longer time to charge (i.e., is more resistive) than did the other three foams. Orange foam appeared to be the least resistant based on its charging time, and the red and yellow appeared to be almost equal in charging time.

3. Figure A.5 indicates the effects on charging time after the foams had been wetted with baseline JP-4 fuel (rest conductivity of 10 pS/m). The charging times decreased considerably, which is attributed to the fuel providing a more conductive path for the charge to travel. Therefore, when foams are wetted with present day (100-200 pS/m) or even baseline (2-10 pS/m) Air Force fuels, it appears that their resistivity decreases.

4. Table A.1 illustrates a comparison of the foams' relaxation rates using the charge decay time constants. Although most values generated during a test fluctuated from the values stated in Table A.1, the same trends were consistently present. Red and yellow foams charge decay times were approximately equal and approximately three to five times greater than the orange, while the blue foam had a relaxation time which was approximately one order of magnitude greater than the red and yellow foam. Similar trends were observed for the fuel wetted foams.

5. Using the ASTM procedure, typical values of resistivity are shown in Table A.2. Again, the trends are obvious and very similar to the trends observed during the foam charge relaxation rate testing. A graph comparing several tests and

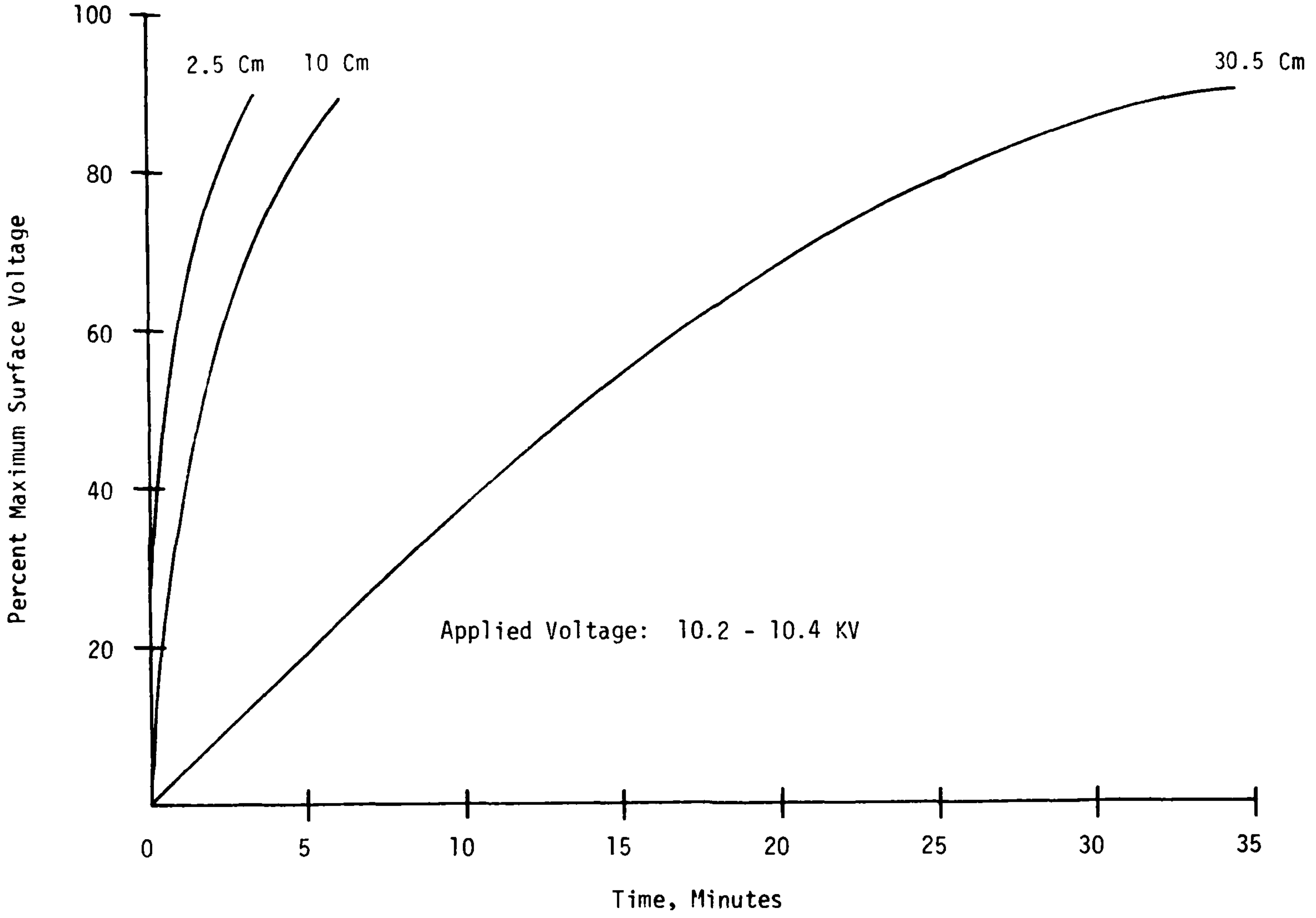

Figure A.3. Effects of Blue Foam Thickness on Surface Charging Time

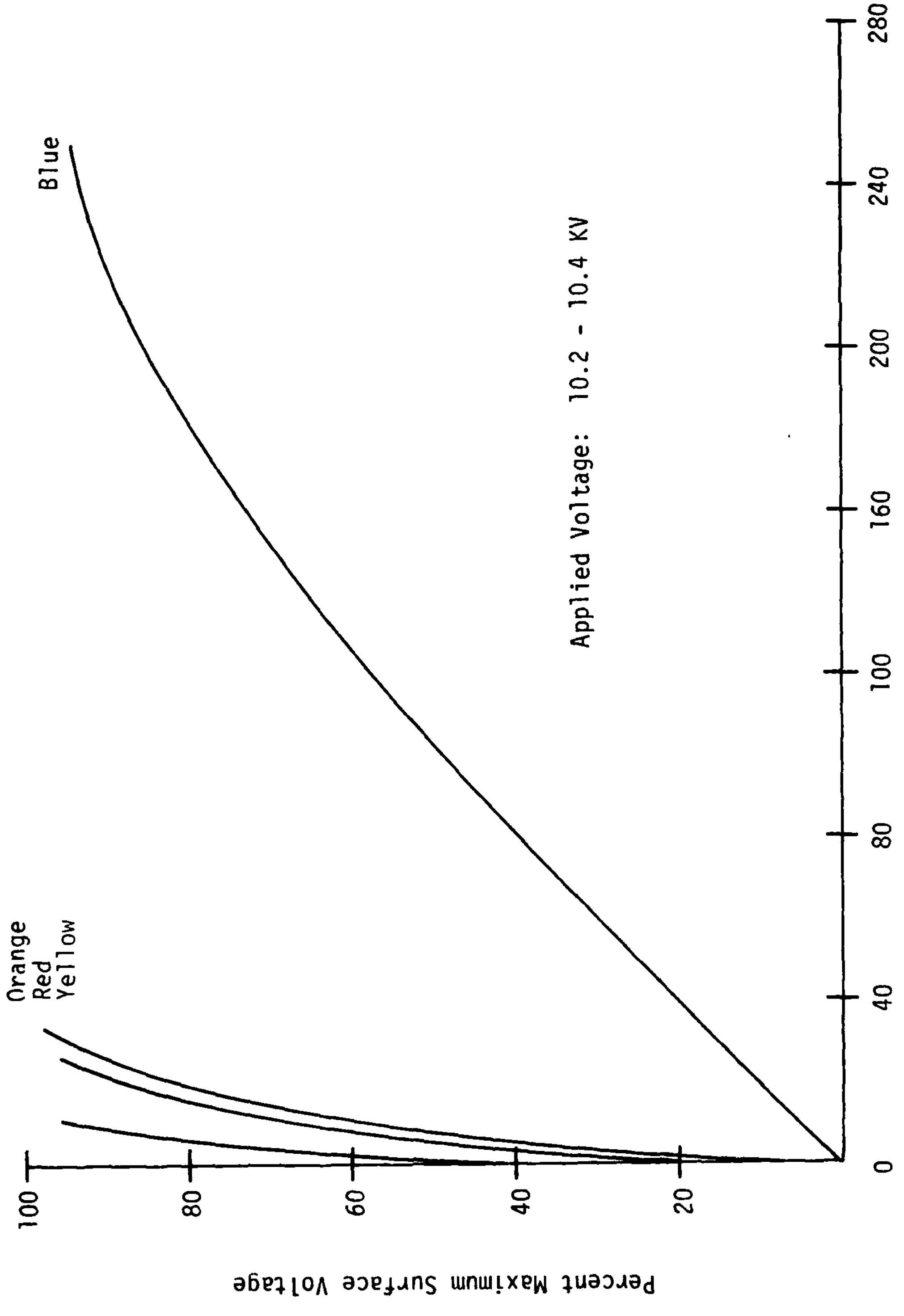

Figure A.4. Comparison of Foam Surface Charging Time for 10 Cm (4 Inch) Thick Dry Foams

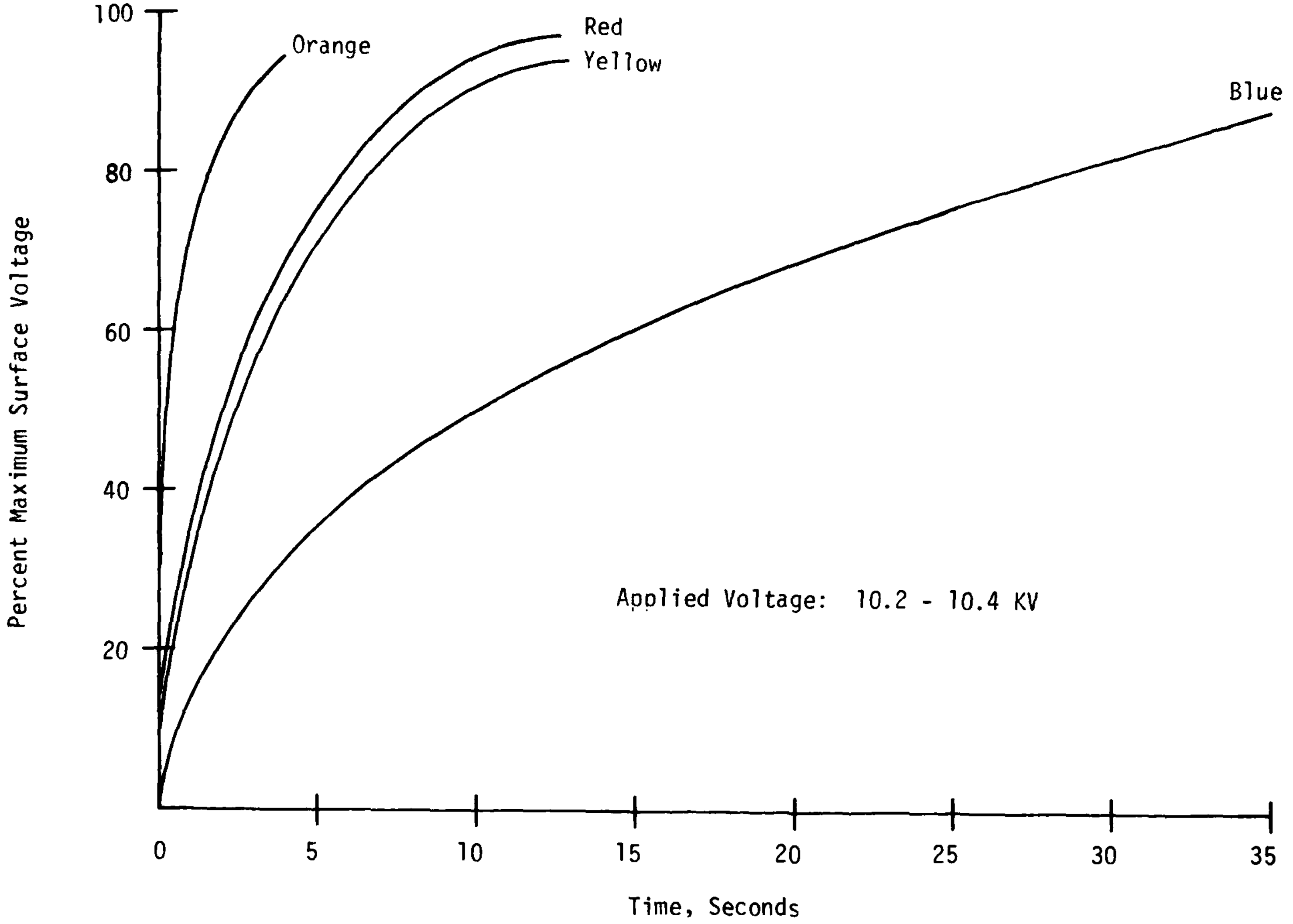

Figure A.5. Comparison of Foam Surface Charging Time for 10 Cm (4 Inch) Thick Wet Foams (10 CU)

TABLE A.1.

COMPARISON OF CHARGE RELAXATION TIME CONSTANTS
FOR 10 Cm THICK FOAM SAMPLES

(Data Obtained from a Typical Test)

Foam Sample	Dry Foam		Fuel-Wetted Foam*	
	τ , Sec.	τ/τ Orange	τ , Sec.	τ/τ Orange
Blue	378	47.3	54	13.5
Yellow	34	4.3	14	3.5
Red	28	3.5	12	3.0
Orange	8	1.0	4	1.0

*Foam Samples were prepared by soaking them in JP-4 (10 pS/m) for 20 minutes followed by draining excess fuel for 20 minutes.

TABLE A.2.

TYPICAL VOLUME RESISTIVITY OF VARIOUS FOAM SAMPLES

Foam Type	Volume Resistivity (Ohm-Cm)			
	Dry Foam (10^{13})	JP-4 Fuel Wetted Foam		
		10 pS/m (10^{13}ohm-cm)	100 pS/m (10^{12}ohm-cm)	1,000 pS/m (10^{11}ohm-cm)
Blue Polyether	400	42.3	37.8	29.4
Red Polyester	35.5	20.9	9.0	10.8
Yellow Polyester	23.4	16.1	16.5	---
Orange Polyester	7.6	2.9	3.5	---

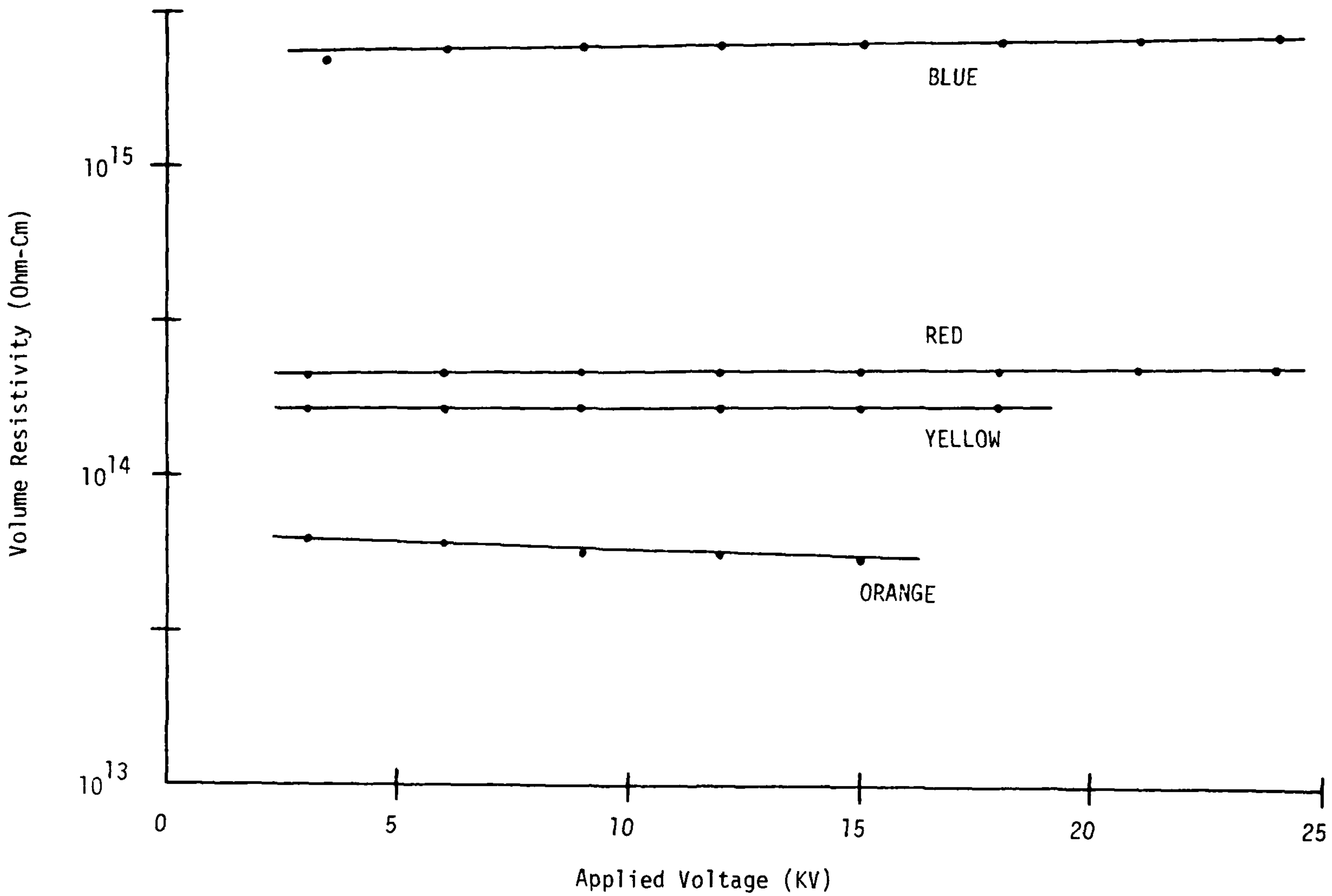

Figure A.6. Effects of Applied Voltage on Foam Volume Resistivity illustrating the ohmic properties of the various foams is shown in Figure A.6. In addition, fuel wetted foam appeared to reduce foam resistivity significantly; however, the conductivity level of the fuel had little effect on the foams' resistivities (Table A.2).

Conclusions

The polyether foam (light blue) had a resistivity in the 10^{15} ohm-cm range, while the polyester foams (red, yellow, and orange) had resistivity values in the 10^{13} to 10^{14} ohm-cm range. While the actual values varied substantially (due to humidity and temperature changes), the trends as stated previously were quite clear. The red and yellow foams were generally three to five times greater than the orange foam, and the blue foam was generally one order of magnitude greater than the red and yellow foams. It can be stated that the resistive nature of the polyurethane foams will permit charge accumulation to occur. The magnitude of charge accumulation taking place will be dependent upon the amount of charge generated and the conductive properties of the foams. Therefore, blue polyether foam would permit more charge accumulation to occur for a given charge generation level than would red, yellow, or orange polyester foams.

APPENDIX B

EXXON MINI-STATIC TEST PROCEDURE (Reference 16)

1.0 Scope

This method is intended to measure the relative static electricity charging tendency of different filter/separator media and/or fuels.

2.0 Summary of Method

The test involves the measurement of static electricity generated by the contact and separation of two dissimilar materials - fuel and filter. Ions of one sign are selectively absorbed on the charge separating surface - the filter, while those of opposite sign are separated and carried along with the flowing fuel. Separated charge is observed by measuring the current that flows to ground from the electrically isolated filter. Level of charge is influenced by filter surface area, filter composition, flow rate, fuel characteristics, and impurities. By holding filter area and flow rate constant, charge level or charge density (charge per unit volume of fuel) becomes an indicator of relative charging tendency between fuels when using the same filter composition or between filter media when using the same fuel. In this test, a measured sample of fuel is forced by means of a syringe/plunger to flow through a filter at a constant flow rate using the mechanical drive of the Minisonic Separometer apparatus. Streaming current off the filter is measured with a Keithley 600B Electrometer.

3.0 Apparatus

The apparatus consists of the following:

3.1 Keithley Electrometer - Model 600B

3.2 Strip Chart Recorder - Hewlett-Packard 7100 Model Series

3.3 Filter Holder - 13mm Dia stainless steel, Swinny, Millipore, Cat. No. NC/1 XX30 01200.

3.4 Valve - Hamilton Valve Co., Part No. 2LF1.

3.5 Receiver - Stainless steel beaker, 600 ml, Ace Chemical Co., Cat. No. 10-3430, EDP-NO-82.

3.6 Syringe/Plunger - Luer-Loc Plastipak Syringe, 50cc, Becton, Dickinson and Co., Rutherford, N.J. (Fisher Scientific Co., Cat. No. 14-823-20).

3.7 Minisonic Separometer Syringe Drive - Emcee Electronics, Wilmington, Delaware. NOTE: Only the syringe drive, holder, and variable speed control power supply of the Minisonic Separator are required for this test.

3.8 Punch - 13mm (1/2") diameter Arch Punch (Gasket cutter) C.S. Osborne Co., Harrison, N.J.

3.9 Tweezers - Suitable clean, dry tweezers shall be used at all times when handling the filter specimens.

3.10 Hard Plastic or Teflon Tubing - 1.6mm (1/16") I.D. approximately by 30 cm to 46 cm long, Eastman Chemical Co.

3.11 Rubber stopper to fit snugly into fuel syringe body.

3.12 Appropriate clamps to hold stopper into syringe body.

3.13 Six-sided Faraday Cage with appropriate entry door.

3.14 Stop watch or timer capable of indicating elapsed time in seconds.

3.15 Above apparatus arranged and connected as shown in Figure B.1. NOTE: Electrical input lead to Keithley and hard plastic tubing should be as short as possible.

4.0 Preparation of Filter Media

4.1 Suitable filter media may be selected for any type of filter paper stock. In addition, specimens may also be prepared from new or used coalescer or separator paper type elements - either of the pleated or cylindrical form.

4.2 When using commercial paper elements, cut open cartridge to be tested using knife, scissors, or snips. Remove a 10-13 cm square of the media. Store in large evaporating dish covered tightly with foil.

> Caution: Handle all media by the edges only, and do not use for test any part that has been soiled or contacted by the hands.

4.3 Punch out about twenty 12.7 mm diameter disks of each material to be tested and place in Petri dish (one dish for each F/S media type). Keep dish covered except in the act of transferring disks.

5.0 Preparation of Test Apparatus

5.1 Cleaning of Fuel Syringe and Filter Holder. Although the Exxon procedure requires the fuel syringe body and entire filter holder to be thoroughly washed between tests with chloroform, purified non-polar cyclohexane (electrical conductivity below 1pS/m) was used instead. Dry in a stream of dry nitrogen.

> Caution: Let parts equilibrate to room temperature before reusing.

5.2 Filter. Load the filter holder base (lower portion) in the following order: flat Teflon washer, support screen, sample filter media, support screen, and Teflon o-ring. Tape threads of top half - to prevent leakage by threads - use Teflon tape. Join halves together finger tight.

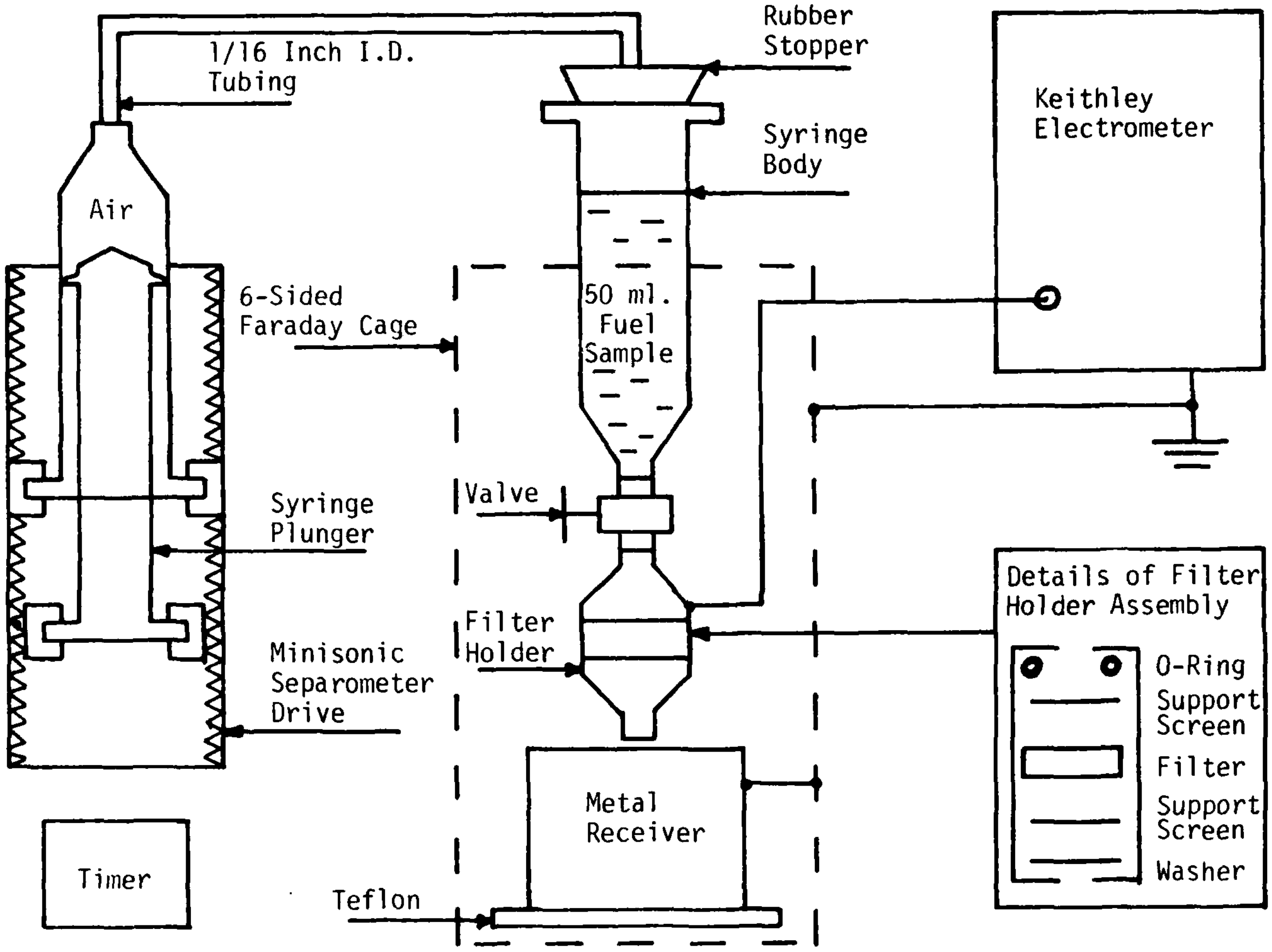

Figure B.1. Mini-Static Charging Test Apparatus

5.3 Apparatus

5.3.1 Check that fuel syringe holder and 600B electrometer are well grounded. Turn 600B on and allow sufficient time for instrument warm-up. Check batteries of electrometer.

5.3.2 Adjust Minisonic Separometer drive potentiometer to obtain fuel flow rate of 100 ml/min during test. Leave drive in UP position.

5.3.3 Apply (occasionally) silicone lubricant to air drive syringe plunger.

5.3.4 Center receiver under filter and connect to ground.

5.4 Syringe

5.4.1 Attach valve to fuel syringe body, turn off. Fill with test fuel to slightly above the 50 ml mark, insert stopper with tubing and place assembled syringe in holder. Clamp stopper to holder.

5.4.2 Attach filter and connect electrometer input to base (lower portion) of filter, avoiding strain on the connection.

6.0 Test Procedure

6.1 Zero the electrometer on the 0.01 multiplier, then set at 0.1 multiplier and 10^{-6} amp range or other settings if known. Unlock the test button.

6.2 Turn drive direction switch DOWN and open the valve. Turn drive ON. Start timer when fuel level passes 50 ml mark.

6.3 After approximately five seconds set electrometer to best reading range using only the 0.1 or 0.3 multiplier but any current range.

> Caution: At this point, remove hands and body from vicinity of filter holder, electrical leads, and Faraday Cage and avoid motion.

6.4 Mark the strip recording when the plunger reaches the 25 to 20 ml mark on the syringe.

6.5 At the end of the fuel flow, turn the drive and timer off.

6.6 Measure the fuel temperature in the receiver.

6.7 Disassemble the syringe and filter holder as soon as possible after recording the data.

6.8 Obtain a repeat measurement by repeating all steps given in Sections 5 and 6.

7.0 Record

7.1 Record the average value of streaming current, in microamperes, between the 25 to 20 ml marks for each run. Also, record the time for 50 ml of fuel to flow through the filter and the sample temperature of fuel in the receiver.

8.0 Calculation and Report

8.1 Calculate the relative charging tendency of filter and/or fuel for each determination as follows:

$$Q = \frac{i}{v}$$

where,

Q = Charge density (microcoulombs/meter^3, $\mu C/m^3 = \mu A$ seconds/m^3)

i = Streaming current (microamperes, μA)

v = Volumetric flow rate (meter^3/second, m^3/second)

8.2 Report the average charge density of the two determinations and the average sample temperature.

APPENDIX C

LARGE-SCALE FUEL FLOW TEST DATA

BASELINE JP-4 FUEL TESTS

Test No.	Fuel No.	Cond.-Charge Tend.-Temp. pS/m-μC/m³-°C	Flow Rate m³/hr. (GPM)	Velocity m/sec. (FPS)	Target Foam Type-No.	Max. Field* Strength KV/m	No. of Discharges >1.5μ Amps	Remarks
1	9		5.2 (23.0)	20.4 (66.8)	Blue-6	284	---	
2	10		5.2 (23.0)	20.4 (66.8)	Blue-7	214	---	
3	11		5.2 (23.0)	20.4 (66.8)	Blue-1	508	144	
4	12	15.4-1742-18	5.2 (23.0)	20.4 (66.8)	Blue-2	386	111	
5	13		5.2 (23.0)	20.4 (66.8)	Blue-3	406	92	
6	14		5.2 (23.0)	20.4 (66.8)	Blue-4	406	92	
7	15		5.5 (24.0)	21.2 (69.7)	Blue-5	386	80	
8	16		5.7 (25.0)	22.1 (72.6)	Blue-6	366	71	
9	17		5.2 (23.0)	20.4 (66.8)	Blue-7	304	58	
10	18		5.2 (23.0)	20.4 (66.8)	Blue-8	182	5	
11	19		5.2 (23.0)	20.4 (66.8)	Blue-9	264	1	
12	20		5.2 (23.0)	20.4 (66.8)	Blue-10	214	3	
13	21	13.1-2403-18	5.2 (23.0)	20.4 (66.8)	Blue-11	254	1	
14	22		5.2 (23.0)	20.4 (66.8)	Blue-12	182	0	
15	1		5.2 (23.0)	20.4 (66.8)	Blue-13	254	0	

*Field Strength Measured 0.05 Meters from Top of Foam Surface

BASELINE JP-4 FUEL TESTS

Test No.	Fuel No.	Cond.-Charge Tend.-Temp. pS/m-μC/m^3-°C	Flow Rate m^3/hr. (GPM)	Velocity m/sec. (FPS)	Target Foam Type-No.	Max. Field* Strength KV/m	No. of Discharges >1.5μ Amps	Remarks
16	2		5.2 (23.0)	20.4 (66.8)	Blue-14	214	0	
17	3		5.2 (23.0)	20.4 (66.8)	Blue-1	498	73	Target Foam Fuel Soaked for 24 Hours for Test 17
18	4		5.2 (23.0)	20.4 (66.8)	Blue-8	264	13	
19	5		5.2 (23.0)	20.4 (66.8)	Blue-9	244	1	
20	6		5.2 (23.0)	20.4 (66.8)	Blue-10	304	0	
21	7		5.2 (23.0)	6.4 (21.1)	Blue-11	204	0	
22	8	9.1-1378-19	5.2 (23.0)	6.4 (21.1)	Blue-1	508	97	Target Foam Fuel Soaked for 48 Hours Before Test 22
23	9		5.0 (22.0)	6.2 (20.2)	Blue-2	498	72	
24	10	5.7-1856-19	5.2 (23.0)	6.4 (21.1)	Blue-3	468	56	
25	11		5.2 (23.0)	6.4 (21.1)	Blue-4	386	33	
26	12		5.2 (23.0)	6.4 (21.1)	Blue-5	284	17	
27	13		5.2 (23.0)	6.4 (21.1)	Blue-6	294	6	
28	14		5.2 (23.0)	6.4 (21.1)	Blue-7	194	1	
29	15		5.2 (23.0)	6.4 (21.1)	Blue-8	214	0	
30	16		5.0 (22.0)	6.2 (20.2)	Blue-9	204	0	

*Field Strength Measured 0.05 Meters from Top of Foam Surface

BASELINE JP-4 FUEL TESTS

Test No.	Fuel No.	Cond.-Charge Tend.-Temp. pS/m-μC/m^3-°C	Flow Rate m^3/hr. (GPM)	Velocity m/sec. (FPS)	Target Foam Type-No.	Max. Field* Strength KV/m	No. of Discharges >1.5μ Amps	Remarks
31	17		5.2 (23.0)	20.4 (66.8)	Blue-10	304	11	Target Foam Rotated 90° for Test 31 thru 33
32	18		5.2 (23.0)	20.4 (66.8)	Blue-11	214	0	
33	19		5.2 (23.0)	20.4 (66.8)	Blue-12	204	1	
34	1		5.2 (23.0)	20.4 (66.8)	Red-1	366	0	
35	2		5.2 (23.0)	20.4 (66.8)	Red-2	386	0	
36	3		5.2 (23.0)	20.4 (66.8)	Red-3	234	0	
37	4		5.2 (23.0)	20.4 (66.8)	Orange-1	102	0	
38	5		5.2 (23.0)	20.4 (66.8)	Orange-2	92	0	
39	6		5.2 (23.0)	20.4 (66.8)	Blue-1	610	144	
40	7		1.8 (8.0)	7.1 (23.2)	Blue-1	204	8	
41	8		0.9 (4.0)	3.5 (11.6)	Blue-1	30	0	
42	9		2.3 (10.0)	8.8 (29.0)	Blue-2	214	0	
43	1		1.8 (8.0)	7.1 (23.2)	Blue-1	102	0	
44	2		5.2 (23.0)	20.4 (66.8)	Blue-2	336	0	
45	3	14.6-541-18	2.3 (10.0)	8.8 (29.0)	Blue-3	204	0	

*Field Strength Measured 0.05 Meters from Top of Foam Surface

BASELINE JP-4 FUEL TESTS

Test No.	Fuel No.	Cond.-Charge Tend.-Temp. pS/m-μC/m^3-°C	Flow Rate m^3/hr.(GPM)	Velocity m/sec.(FPS)	Target Foam Type-No.	Max. Field* Strength KV/m	No. of Discharges >1.5μ Amps	Remarks
46	4		5.5 (24.0)	21.2 (69.7)	Blue-4	172	0	
47	6	12.0-314-19	5.5 (24.0)	21.2 (69.7)	Blue-2	330	3	
48	7		5.5 (24.0)	21.2 (69.7)	Blue-3	194	0	
49	8		3.2 (14.0)	12.4 (40.7)	Blue-1	406	14	
50	9	13.1- -18	3.2 (14.0)	12.4 (40.7)	Blue-2	234	31	
51	10		3.2 (14.0)	12.4 (40.7)	Blue-3	204	4	
52	11		2.0 (9.0)	8.0 (26.1)	Blue-4	76	0	
53	12		5.9 (26.0)	23.0 (75.5)	Blue-5	468	0	
54	13		2.3 (10.0)	8.8 (29.0)	Blue-1	304	73	
55	14		1.8 (8.0)	7.1 (23.2)	Blue-1	224	31	
56	15	10.8-1456-19	1.7 (7.5)	6.6 (21.8)	Blue-1	254	62	
57	16	9.1-746-18	1.4 (6.0)	5.3 (17.4)	Blue-1	174	12	
58	17	8.0-2013-18	6.1 (27.0)	7.6 (24.8)	Blue-1	406	106	
59	18	8.6-1652-20	4.5 (20.0)	5.6 (18.4)	Blue-1	336	186	
60	19	7.4-1602-18	3.6 (16.0)	4.5 (14.7)	Blue-1	326	46	

*Field Strength Measured 0.05 Meters from Top of Foam Surface

BASELINE JP-4 FUEL TESTS

Test No.	Fuel No.	Cond.-Charge Tend.-Temp. pS/m-μC/m^3-°C	Flow Rate m^3/hr.(GPM)	Velocity m/sec.(FPS)	Max. Field* Strength KV/m	No. of Discharges >1.5μ Amps	Remarks
61	20	7.4-1554-18	2.5 (11.0)	3.1 (10.1)	40	0	Tests were Conducted with New Blue Target Foam Sections
62	21		2.7 (12.0)	3.4 (11.0)	122	1	
63	22	14.0-2800-17	1.8 (8.0)	2.2 (7.3)	122	0	
		10.3-2500-17					
64	1		1.8 (8.0)	2.2 (7.3)	70	0	
65	2	5.1-618-20	2.8 (12.5)	3.5 (11.5)	72	0	
66	3		3.6 (16.0)	4.5 (14.7)	150	0	
67	4	3.4-781-20	4.4 (19.5)	5.5 (17.9)	274	1	
68	5		5.2 (23.0)	6.4 (21.1)	366	56	
69	6	6.3-405-17	6.4 (28.0)	7.8 (25.7)	440	36	
70	7		5.5 (24.0)	6.7 (22.0)	398	58	
71	8	7.4-1170-17	5.0 (22.0)	6.2 (20.2)	346	33	
72	9	5.7-2016-17	3.5 (15.5)	4.3 (14.2)	284	20	
73	10	5.1-1310-18	3.0 (13.0)	3.6 (11.9)	182	0	
74	11	4.9-1088-18	1.8 (8.0)	2.2 (7.3)	204	0	

* Field Strength Measured 0.05 Meters from Top of Foam Surface

BASELINE JP-4 FUEL TESTS

Test No.	Fuel No.	Cond.-Charge Tend.-Temp. pS/m-μC/m^3-°C	Flow Rate m^3/hr. (GPM)	Velocity m/sec.(FPS)	Target Foam Type-No.	Max. Field* Strength KV/m	No. of Discharges >1.5μ Amps	Remarks
75	12	2.9-1209-13	5.3 (23.5)	20.8 (68.3)	Blue-1	406	159	
76	13	3.7-942-12	5.3 (23.5)	20.8 (68.3)	Red-1	112	0	
77	14	5.1-1546-14	5.2 (23.0)	20.4 (66.8)	Blue-1	498	113	Target Foam Treated with Methanol for Tests 77 and 78
78	15	5.7-1148-13	5.2 (23.0)	20.4 (66.8)	Blue-2	630	102	
79	16	6.3-1472-11	5.2 (23.0)	20.4 (66.8)	Blue-1	508	123	Void Configuration Changed for Tests 79, 80, and 81
80	18	5.7-1599-12	1.8 (8.0)	7.1 (23.2)	Blue-1	220	967	
81	19	6.3-1715-13	5.5 (24.0)	21.2 (69.7)	Blue-2	336	---	
82	20	5.7-1649-16	5.3 (23.5)	20.8 (68.3)	Blue-1	478	---	Number of Discharges for Those Tests Showing a Dashed Line Was Not Determined (>1000)
83	21	5.1-1973-	5.2 (23.0)	20.4 (66.8)	Blue-1	406	---	
84	22	8.8-2083-13	5.5 (24.0)	21.2 (69.7)	Blue-1	406	---	
85	23	6.6-1863-13	5.5 (24.0)	21.2 (69.7)	Blue-1	468	---	
86	24	8.0-2017-13	5.5 (24.0)	21.2 (69.7)	Blue-1	488	---	
87	25	6.3-2795-13	6.4 (28.0)	7.8 (25.7)	Blue-1	488	77	

*Field Strength Measured 0.05 Meters from Top of Foam Surface

FUEL CONDUCTIVITY ADDITIVE TESTS (ASA-3)

Test No.	Fuel No.	Cond.-Charge Tend.-Temp. pS/m-μC/m^3-°C	Flow Rate m^3/hr. (GPM)	Velocity m/sec. (FPS)	Max. Field* Strength KV/m	No. of Discharges >1.5μ Amps	Remarks
88	26	22.8-2434-14	5.3 (23.5)	20.8 (68.3)	498	361	ASA-3 Added Before Tests 88, 92, 94, and 99
89	27	18.3-2229-18	5.5 (24.0)	21.2 (69.7)	610	---	Tests were Conducted with New Blue Target Foam Sections
90	28	18.3-1226-17	6.4 (28.0)	7.8 (25.7)	660	190	
91	29	17.1-1245-16	6.4 (28.0)	7.8 (25.7)	498	---	
92	30	30.8-3600-18	5.9 (26.0)	7.3 (23.9)	488	295	
93	31	36.0-3600-20	6.1 (27.0)	7.6 (24.8)	508	---	
94	32	74.2-5061.20	5.2 (23.0)	20.4 (66.8)	386	222	
95	33	74.2-5061-20	5.2 (23.0)	6.4 (21.1)	304	---	
96	34	159.9-8772-21	5.9 (26.0)	7.3 (23.9)	10	0	
97	35	119.9-6226-19	6.0 (26.5)	7.4 (24.3)	216	6	
98	36	119.9-6972-19	6.0 (26.5)	7.4 (24.3)	50	0	
99	37	97.0-4920-17	5.2 (23.0)	20.4 (66.8)	30	0	
100	38	137.0-7150-14	5.2 (23.0)	20.4 (66.8)	50	0	Tests were Conducted with New Blue Target Foam Sections
101	39	102.8- -19	4.5 (20.0)	17.7 (58.1)	346	172	
102	40	105.6-6396-19	5.0 (22.0)	19.5 (63.9)	354	106	

*Field Strength Measured 0.05 Meters from Top of Foam Surface

FUEL PROSTATIC ADDITIVE TESTS (GULF-178)

Test No.	Fuel No.	Cond.-Charge Tend.-Temp. pS/m-μC/m^3-°C	Flow Rate m^3/hr.(GPM)	Velocity m/sec. (FPS)	Gulf-178 (PPM)	Max. Field* Strength KV/m	No. Of Discharges >1.5μ Amps	Remarks
103	1		4.5 (20.0)	17.7 (58.1)	0	82	0	Tests were Conducted with New Blue Target Foam Sections
104	2	2.0-56.5-18	5.0 (22.0)	19.5 (63.9)	0	170	3	
105	3	2.0- -19	5.0 (22.0)	19.5 (63.9)	0	182	6	
106	4	2.6- -18	5.2 (23.0)	20.4 (66.8)	40	40	0	
107	5	3.5-112-19	5.2 (23.0)	20.4 (66.8)	79	82	0	
108	6	5.3-126-18	4.8 (21.0)	18.6 (61.0)	119	82	0	
109	7	6.0-391-18	5.1 (22.5)	19.9 (65.4)	159	-92	0	
110	8	7.7-517-18	5.1 (22.5)	19.9 (65.4)	198	-172	0	
111	9	8.6- -18	5.0 (22.0)	19.5 (63.9)	238	-162	0	
112	10	9.1- -18	5.2 (23.0)	20.4 (66.8)	277	-234	0	Test 113 was Void Due to Operator Error
114	12		5.3 (23.5)	20.8 (68.3)	317	-336	0	
115	13		5.3 (23.5)	20.8 (68.3)	357	-336	0	
116	14		5.2 (23.0)	20.4 (66.8)	357	-100	0	
117	15	14.3-2351-18	5.3 (23.5)	20.8 (68.3)	396	-132	0	
118	1		5.2 (23.0)	20.4 (66.8)	0	152	---	Fuel Tank Top Blue Foam Piece Changed to 3" Thick Section for Tests 118 Thru 122

*Field Strength Measured 0.05 Meters from Top of Foam Surface

FUEL PROSTATIC ADDITIVE TESTS (GULF-178)

Test No.	Fuel No.	Cond.-Charge Tend.-Temp. pS/m-μ C/m3-°C	Flow Rate m^3/hr. (GPM)	Velocity m/sec. (FPS)	Gulf-178 (PPM)	Max. Field* Strength KV/m	No. of Discharges >1.5μ Amps	Remarks
119	2	6.3-243-19	5.3 (23.5)	20.8 (68.3)	0	426	0	Tests were Conducted with New Blue Target Foam Sections
120	3	2.9-180-19	5.3 (23.5)	20.8 (68.3)	396	-152	0	
121	4	5.4-777-18	5.3 (23.5)	20.8 (68.3)	396	-182	0	
122	5	7.4-1386-18	5.2 (23.0)	20.4 (66.8)	793	-138	0	
123	6	10.3-1783-19	5.3 (23.5)	20.8 (68.3)	1189	-316	41	Fuel Tank Top Blue Foam Piece Changed Back to 4" Thick Section for Tests 123 Thru 129
124	7	14.8-3140-18	5.5 (24.0)	21.2 (69.7)	1585	-966	594	
125	8	17.1-3296-19	5.5 (24.0)	21.2 (69.7)	1585	-966	560	New Red Target Foam
126	9	18.8-3490-20	5.5 (24.0)	21.2 (69.7)	1585	-812	202	New Orange Target Foam
127	10	20.7-3960-18	5.5 (24.0)	21.2 (69.7)	1585	-1016	---	
128	11	20.6-3388-18	5.0 (22.0)	19.5 (63.9)	1585	-1016	---	
129	12		5.5 (24.0)	21.2 (69.7)	1585	-1016	---	

*Field Strength Measured 0.05 Meters from Top of Foam Surface

FUEL CONDUCTIVITY AND PROSTATIC ADDITIVE TESTS (ASA-3/GULF-178)

Test No.	Fuel No.	Cond.-Charge Tend.-Temp. pS/m-μC/m^3-°C	Flow Rate m^3/hr. (GPM)	Velocity m/sec. (FPS)	Max. Field* Strength KV/m	No. of Discharges >1.5μ Amps	Remarks
130	13		5.2 (23.0)	20.4 (66.8)	-122	0	Gulf-178 Concentration was 1585 PPM by Volume for All Tests
131	14	94.2-4824-18	5.2 (23.0)	20.4 (66.8)	-204	0	
132	15	119.9-4956-18	5.2 (23.0)	20.4 (66.8)	-204	0	Tests were Conducted with New Blue Target Foam Sections
133	16	99.9-4368-19	5.2 (23.0)	20.4 (66.8)	-102	0	
		94.2-4444-18					
134	1		5.2 (23.0)	20.4 (66.8)	0	0	
135	2	4.4-110-18	5.2 (23.0)	20.4 (66.8)	0	0	
136	3	2.3-145-18	5.2 (23.0)	20.4 (66.8)	-712	341	
137	4	13.1-1197-19	5.3 (23.5)	20.8 (68.3)	-650	262	
138	5	32.0- -18	5.5 (24.0)	21.2 (69.7)	-712	0	
139	6	51.4- -18	5.0 (22.0)	19.5 (63.9)	-508	0	
140	7	57.1- -18	5.0 (22.0)	19.5 (63.9)	-406	0	
		57.1- -19					

*Field Strength Measured 0.05 Meters from Top of Foam Surface

APPENDIX D

MONSANTO RESEARCH CORPORATION CHEMICAL ANALYSIS OF FUEL/FOAM ADDITIVES (Reference 17)

OBJECTIVE AND METHOD

Samples of reticulated polyurethane foams were analyzed to determine the effect extractable and/or sorbed substances may have on electrostatic charge separation/accumulation activity. This encompassed characterizing and quantifying the substances, either extracted and/or sorbed by the polyurethane foams, that may affect its electrical conductivity.

The foam samples included a new untreated polyether-type polyurethane foam sample (Sample 1), a polyether-type polyurethane foam sample which had experienced fuel impingement upon it (Sample 2); and a new untreated polyester-type polyurethane foam sample (Sample 3). A number of analyzing techniques were used to characterize the fuel/foam interaction phenomena that occurred during refueling testing. They included the following:

Microscopic Examination

The microscopic examination of foam surfaces was conducted with an American Optical Company Series L10 stereomicroscope, equipped with a Polaroid camera. Magnifications of X20, X200, and X10,000 were used.

Gas Chromatographic - Mass Spectrometric (GC-MS) Analysis

The GC-MS analysis with solutions of materials extracted from the foams was performed with a Hewlett-Packard system, Model 5982-A. Two sets of chromatographic conditions were used:

(1) 32 cm x 183 cm (1/8" x 6') glass column, packed with Tenax GC. Starting temperature 80°C. Heated at the rate of 16°C/min., and maintained at 280°C for 20 min. Helium flow rate 30 cc/min.

(2) .32 cm x 183 cm (1/8" x 6') glass column, packed with 3% Dexsil 400 on Chromasorb W. Starting temperature 80°C. Heated at the rate of 16°C/min., and maintained at 280°C for 20 min. Helium flow rate 30 cc/min.

The Tenax column and the conditions applied during its use provided the better results in the resolution of organic extractable materials.

Direct Insertion Probe (DIP) Mass Spectrometric Measurements

Methanol (2 ml), used as the solvent for the extraction, was evaporated. The extracted materials were redissolved in methylene chloride (0.2 ml). Small quantities of the resulting solutions were transferred onto the direct inlet probe, that was inserted into the mass spectrometer cavity. The probe was permitted to heat up to the source temperature (180°C). It was subsequently heated up to 300°C in one minute. Mass spectral fragmentation patterns were reported in 30-second intervals for the first five minutes, in 1-minute intervals for the following five minutes, and finally at the end of the 15-minute probe heating period.

Infrared Spectrometric Measurements

The infrared spectra of the extracted substances, remaining upon evaporation of the solvents on KBr plates, were recorded with a Perkin-Elmer Model 137B Infracord spectrometer.

Thermogravimetric Analysis

The thermogravimetric analysis of the polyether-based polyurethane foam was conducted with a modified American Instrument Company apparatus. A 200-mg sample was used. The sample was heated in helium atmosphere at the rate of 3°C/minute. Onset of degradation was detected at 210°C.

RESULTS

The substances extracted from the polyurethane foams were summarized in Table D.1. From the infrared spectrometric analysis the absorption bands at 5.8 μm and 7.9 μm (see arrows in Figure D.1) are stronger with the materials extracted from the untreated, new polyether foam sample. These are strong characteristic bands of diethylhexyl phthalate. The polyether foam sample which experienced fuel impingement exhibited very strong absorption at 2.9 μm which is attributed to the alkylphenol type substances extracted by the foam sample from the jet fuel (JP-4). This substance was also detected mass spectrometrically.

CONCLUSIONS

It was determined by instrumental analysis that the two most significant compositional changes that occur during the fuel flow testing of the foams with JP-4 are:

- Removal of diethylhexyl phthalate from the foam.

- Absorption of alkylphenol type compounds by the foam.

The latter of these compositional changes is believed to have a relatively larger effect on the polarization characteristics of the foam surface and its conductivity, which could account for the diminishing static discharge occurrence with repetitive JP-4 flow through the foam.

TABLE D.1

SUBSTANCES EXTRACTED FROM POLYURETHANE FOAMS[a,b]

Sample Number	1		2[c]	3[c]
Sample Description	Untreated Blue Foam		Fuel-Extracted Blue Foam	Red Foam
Substance Extracted	Methanol Extract	Pentane Extract		
Tolylene Diisocyanate	0.12	0.0034	0.14	0.041
Methyl Benzimidazolin-2-one	0.042		0.075	0.014
Toluenediamine	0.0086		0.015	
Diethylhexyl Phthalate	0.12	0.15	0.0027	
2,4-Dimethyl-6-*t*-butylphenol	0.099	0.015	0.13	
Unknown[d]				~0.92

[a] The amounts of extracted materials are reported in weight percent, based upon sample weight.

[b] Foam samples (0.23 to 0.30 g) extracted with either methanol or pentane (2 ml) by mechanical shaking for one hour.

[c] Methanol used for extraction.

[d] On the basis of mass spectrometric analysis, the probable molecular weight of this substance is 173.

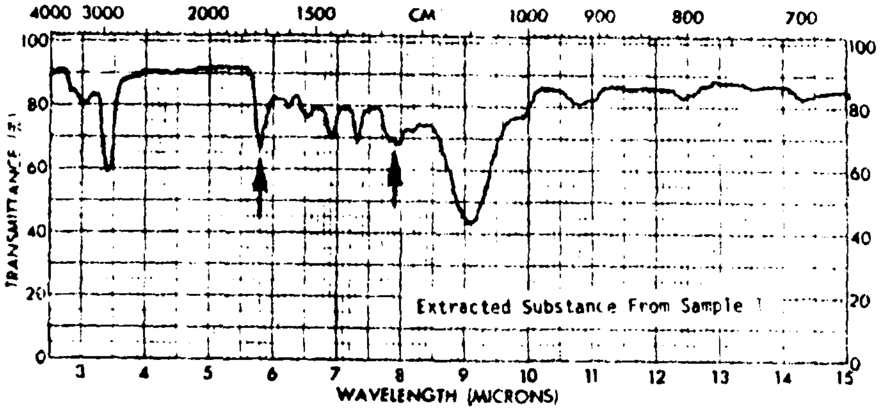

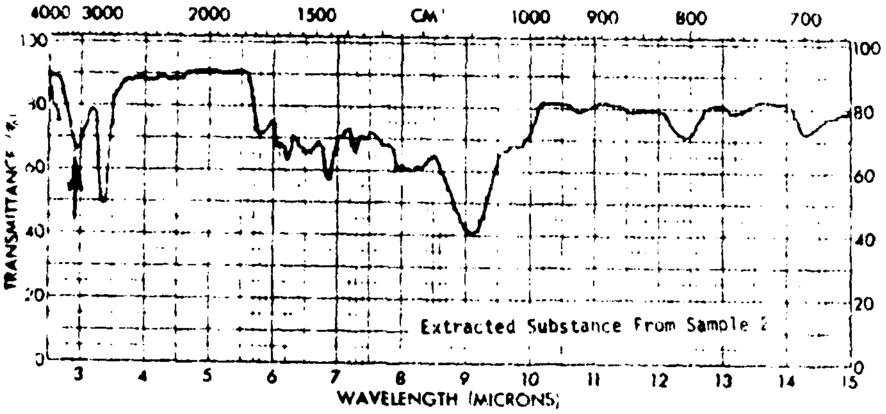

Figure D.1. Infrared Specta of Substances Extracted from Samples 1-2

APPENDIX E

FUEL TANK STATIC ELECTRICITY INCIDENTS REPORTED BEFORE 1978 (PRIOR TO INCORPORATION OF A CONDUCTIVITY IMPROVEMENT ADDITIVE)

(Reference 18)

INCIDENT #1

The F-5E aircraft involved was undergoing initial single point refueling tests with a no-flow nozzle pressure of 410-480 KPa (45-55 psig) when flow to the internal tanks was initiated. After addition of 850 liters (225 gallons), a rush of air and a visible discharge of dust or vapor from the vent opening in the vertical stabilizer was observed. The refueling operation was stopped and inspection through the gravity filler openings in the tank showed no damage. Fueling was completed without further incident.

The fuel probe, yellow foam (TYPE II), and some fuel system components were removed from the forward tank (left fuel system) for examination. The upper portion of the fuel cell (Uniroyal Nitrile Bladder) was sooted from exposure to a flash fire. The yellow foam exhibited charring and sooting along the sides and edges of voided areas, between foam blocks, and between foam and tank wall passages. The vent system had a powdery grayish colored substance along its entire length from the forward tank to the vertical stabilizer. All grounding cables and connections were in good condition and resistances were within tolerances. The boost pump and associated wiring were discountable as a potential ignition source since the system was entirely submerged in fuel. Board findings indicated that the probable cause of the mishap was the ignition of a flammable mixture of fuel and air by a spark discharge. The spark discharge was believed to have been produced by the accumulation of the electrostatic charge in the fuel, possibly occurring between the fuel probe case and the adjacent fuel tank fitting.

INCIDENT #2

The fuel tanks on the F-5E aircraft were being purged with a purging fluid mixture of JP-5 and 1010 oil. After adding 150 liters (40 gallons) of purging fluid to the forward tank (through an over-the-wing hand-held nozzle) a ball of flame erupted on the fuselage approximately a half of meter (two feet) behind the rear tank. The flames were quickly extinguished with CO_2 which limited the damage to blistered paint on the fuselage. It was the opinion of the investigators that ignition occurred at the forward tank opening and propagated rearward due to the effect of wind velocity. The result was the ignition of residual JP-4 fuel vapors coming from the rear tank opening. Continuity readings on the grounding system were determined to be adequate.

INCIDENT #3

After pumping approximately 65 liters (17 gallons) of JP-4 fuel into the UH-1N helicopter's orange foam (TYPE I) packed fuel tank, a loud pop was heard followed by flames shooting out of the right auxiliary fuel tank. Maintenance on the aircraft auxiliary fuel tank had not been performed since installation. Investigation of all grounding points on the ramp, the aircraft, and the refueling truck revealed that the ramp grounding point was corroded and that the aircraft ground attachment point was not free of paint.

INCIDENT #4

Approximately 250 liters (66 gallons) of JP-4 had been transferred to the UH-1N helicopter when a white-orange flame exited from the filler neck opening and continued to burn. The flames were put out with an A-20 fire extinguisher before the tank sustained damage. No noises preceded ignition and there were no sources of sparks or open flame in the area. The helicopter and refueler were bonded but not grounded in accordance with applicable tech orders.

INCIDENT #5

The F-105D was being refueled with JP-4 when white-gray smoke or vapor was observed in the sabre drain. This observation was noted after 1300 liters (343 gallons) had been transferred to the aircraft. Refueling of the aircraft was immediately discontinued and the aircraft impounded for inspection. The sabre drain vent line was examined. Deposits of soot were discovered throughout the line. Inspection of the polyurethane foam (orange, TYPE I) surrounding the mouth of the vent line in cell 3A revealed fire damage consistent with a flash fire of short duration. Due to the location of the damage, all sources of ignition were ruled out except for static electricity. The grounding equipment was found to be functioning properly and the entire refueling operation was conducted in accordance with applicable tech orders.

INCIDENT #6

An F-105F was being refueled with a single point connection at 340 KPa (35 psig) when very slight smoke or vapor was seen coming from the sabre vent drain. Inspection of the orange foam in cells 1A and 3A showed only traces of singeing in cell 1A where fuel enters the tank. Damage was not sufficient to require replacement of the foam or cell. The aft fuselage ground receptacle on the aircraft was determined to be defective. Estimated fuel flow rate was between 70-90 m^3/hr (300-400 gpm).

INCIDENT #7

During the initial refueling stage of the A-10, smoke or condensation was observed coming from the vent boom. Due to this observation, the refueling of the A-10 aircraft was terminated. The access cover of the forward main tank was then removed revealing heat blistering of its inner surface. Soot was observed on the fuel gaging probe approximately 46 Cm (18 inches) above the bottom of the probe. Removal of the red foam sections indicated that widespread fire propagation within the fuel cell had occurred. No damage to the foam or vent line in the aft fuel cell was found. There was no indication of fire in the vent outlet areas in any of the wing tanks. The Wiggens coupling (outer ring) appeared to have been electrically insulated due to the heavy anodized coating, and it was believed that this electrical isolation acted as the charge collector.

INCIDENT #8

After having been fueled and defueled once, an A-10A was being refueled for the second time, when smoke and pieces of red foam were noticed in the aircraft fuel vent mast. The aircraft was being fueled in accordance with previously established procedures entailing reduced flow rates at 205 KPa (15 psig). Investigation revealed that a fire was initiated in the right main (forward) fuselage tank and propagated to the vent collector tank where the flame was suppressed by red foam. Heat and a pressure pulse from the flame front melted a portion of the foam in the vent tank and forced small pieces of foam material into the mast exit. Inspection of the remaining three tanks showed no evidence of flame propagation to these areas. The right main fuel tank pump/can installation experienced an internal explosion resulting in fractures along welds in the top portion of the can. The pump/can assembly was not totally submerged when the electrostatic incident occurred.

U.S. Government Printing Office: 1986 — 646-067/40758